Poly(ester-urethane) Foams for Bone Repair. An *in vitro* degradation Study.

Markus Glarner, Ladina Fliri, Markus Windolf, Mauro Alini, David Eglin

[1] *AO Research Institute, Davos, Switzerland.*

INTRODUCTION: For the healing of large bone defects, scaffold construct should accommodate micro-movements (compression) and maintain the construct-bone tissue contact under load. This is potentially important for the mechanical stimulation of seeded cells and stability of the repair solution in the defect. We report in this study, the first 1.5 year *in vitro* degradation of elastomeric poly(ester-urethane) (PU) scaffolds.

METHODS: The poly(ester-urethane) made of poly(ε-caprolactone) diol (MW=530 $g.mol^{-1}$) hard segment and 1,4,3,6-dianhydro-D-sorbitol soft segment linked with 1,6-hexamethylene diiscyanate was synthesized and the PU and nano-hydroxyapatite particles (nHA, Biomaterials US Ltd., particles size 50-100 nm)/PU scaffolds with pore size average of 200 μm were prepared as previously reported [1]. *In vitro* degradation was achieved by soaking cylindrical 16x8 mm scaffolds in phosphate-buffered saline (PBS), pH 7.4, 37ºC, solution:scaffold w/w ratio equal to 20:1 (ASTM F1635-04a). PBS Solutions and scaffolds were collected at intervals and subjected to pH measurement, weight loss analysis, size exclusion chromatography, viscosimetry measurement, scanning electron microscopy and micro-computed X-ray tomography analysis. Finally, a mechanical test was designed to give a characteristic fingerprint of the viscoelastic foam properties by measuring the scaffolds damping coefficient, stiffness at 30% and 55% strain and relaxation.

RESULTS: For the duration of the in vitro study, no significant variations of pH were measured. Macro-structural parameters (e.g. porosity, pore size, wall thickness) calculated from X-ray tomography reconstructions remained constant except for an initial increase of wall thickness (Δ = 7 μm) at 1 month for the nHA/PU scaffold, indicating slight swelling of the foam. Stiffness values (30% strain) showed an increase of 30% with maximum at 6 months (1.4 ± 0.1 N/mm) and 4 months (3.1 ± 0.5 N/mm) for the PU and nHA/PU scaffolds respectively. Compared to poly(ε-caprolactone) scaffolds with constant Mv as far as 6 months, PU and nHA/PU scaffolds showed 20% decrease of their Mv as early as 4, respectively 1 month, Figure 1.[2]

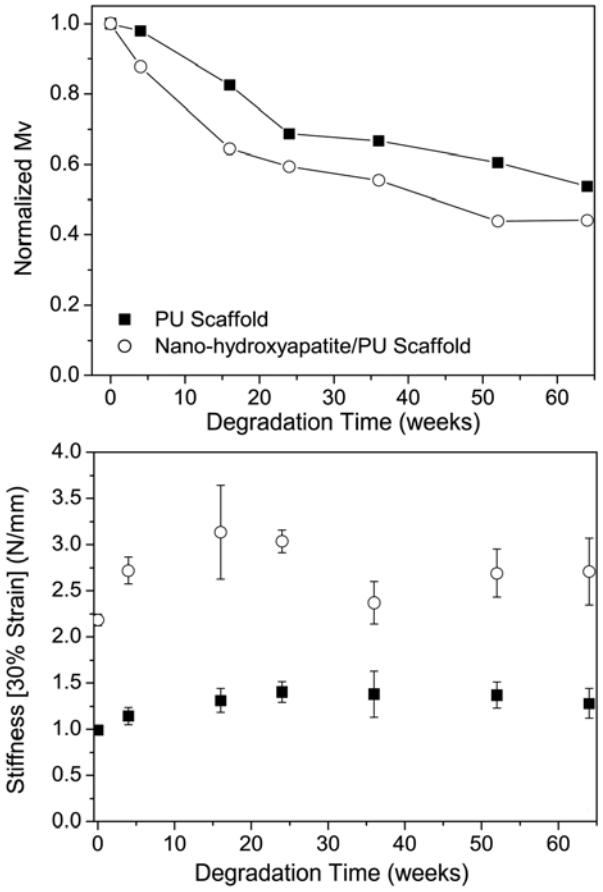

Fig. 1: Plots of PU and nHA/PU foams stiffness and PU Mv values as a function of the degradation time in vitro.

DISCUSSION & CONCLUSIONS: Biodegradable poly(ester-urethane) based scaffolds are able to keep their initial structural and mechanical properties for more than 9 months *in vitro*, making them suitable constructs for the healing of challenging large bone defect. Addition of nHA modulates the initial mechanical properties and osteoconductivity of the scaffold [1] without modifying significantly the rate of degradation.

REFERENCES: [1] Carole IR Boissard et al. Acta Biomater (9):3316-27 2009. [2] Christopher XF Lam, et al. J Biomed Mater Res A. 90(3):906-19 2009.

Adherent endotoxins on bone implant surfaces: a reappraisal

M. Morra, C. Cassinelli, D. Bollati, G. Cascardo

Nobil Bio Ricerche, Via Valcastellana 26, 14037, Portacomaro (AT), Italy

INTRODUCTION: Osteoimmunology, i.e. the cross-talk between cells from the immuno and skeletal systems, suggests a role of pro-inflammatory citokines in the stimulation of osteoclasts activity [1]. Adherent endotoxin challenges to inflammatory cells are directly relevant to implant pathologies involving bone resorption, such as osteointegration failure, aseptic loosening and periimplantitis. Endotoxin amount on implant devices is regulated by standards, but it is not known whether commercially available bone implants elicit different levels of adherent-endotoxins stimulated cytokines. The objective of this work is to develop a model system and to evaluate the expression of pro-inflammatory citokines genes relevant to osteoclasts activation (IL-1, IL-6, TNFα) on several clinically available bone implant devices.

METHODS: To validate the method, murine J774-A2 macrophages were cultured on Ti disks with different level of Lipopolysaccharide (LPS) contamination, to define the time-course of the inflammatory response to endotoxins, as evaluated by RT-PCR analysis. Peak expression of IL-1, IL-6, TNFα at 4 h culture was shown to be directly related to the amount of adherent endotoxin. Gene expression at 4 h was then measured on several commercially available dental implants, and on self-tapping fixation bone screws packaged, sterile, that is in the "as-implanted" condition.

RESULTS: Adherent endotoxins induce different expression of genes involved with the stimulation of osteoclast activity on the tested implant devices. Results are not affected by the specific surface treatment, rather they likely reflect cares in cleaning and packaging protocols. As an example, Fig. 1 shows RT-PCR results obtained on fixation screws, from two different producers (screw 1-2 Vs screw 3-4). The figure contains also data obtained on our negative control, an endotoxin-free Ti disk (Ti control) and our positive control, a Ti disk purposely contaminated by overnight immersion in 1 µg/mL LPS aqueous solution (LPS contaminated Ti control). The graph shows that a clinically "ready to be used" fixation screw elicits up to 400 fold expression of IL-6 as compared to a properly endotoxin-cleaned Ti sample. Inflammatory gene expression for fixation screw 1 and 2 are respectively much higher and similar to that observed on positive control. This level of contamination has been shown to induce significant osteoclast activation, *in vitro* and bone resorption, *in vivo* [2].

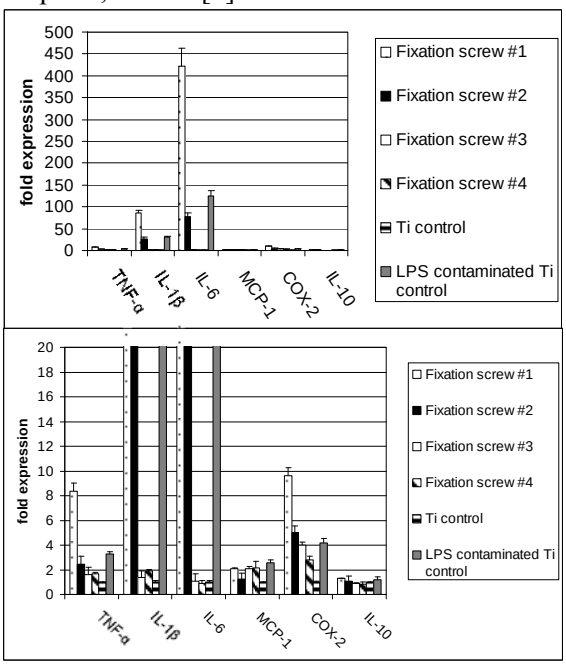

Fig. 1: RT-PCR measurement of gene expression by J774-A2 macrophages cultured on fixation screws (two different vertical scales are used for clarity).

DISCUSSION & CONCLUSIONS: Expression of genes that enhance osteoclasts activity through endotoxins stimulation of inflammatory cells is widely different on commercially available dental implants and fixation screws, taken as representative examples of bone implant devices. In some case, detected levels are at or above the values known to induce *in vivo* effects. Pathologies such as "aseptic loosening" are nowadays discussed in terms of adherent endotoxins rather than response to particle and materials debris. A reappraisal of the clinical impact of adherent endotoxins on bone implant devices is required, due to the increasing knowledge on crosstalk between cells from the immuno and skeletal systems

REFERENCES: [1] Nakashima, T, Takayanagi H, (2009), J Clin Immunol 29:555–567, [2] Bi, YM et al., (2001) J Bone Miner Res 16:2082–2091,

IN VITRO BACTERIAL ADHESION TO PEEK TAILORED FOR OSSEOINTEGRATION BY SURFACE MODIFICATION

E.T.J. Rochford[1,2], T.F.Moriarty[1], R.G.Richards[1,2], A.H.C.Poulsson[1]

[1] AO Research Institute, Davos, Switzerland. [2]Aberystwyth University, UK.

INTRODUCTION: Increasing the surface energy of polyetheretherketone (PEEK) by oxygen plasma surface treatment has been shown to enhance human primary osteoblast cytocompatibility by increasing surface energy[1]. Altering surface energy causes a change in the binding and conformation of proteins, which can promote eukaryotic cell adhesion[2]. The surface treatment may also affect bacterial adhesion by altering surface chemistry and etching the material surface. This *in vitro* study compares the adhesion of clinically relevant bacteria to untreated PEEK versus oxygen plasma treated PEEK in both a protein free and a blood plasma preconditioned model.

METHODS: Injection moulded PEEK-OPTIMA® discs (Invibio Biomaterial Solutions, UK) were oxygen plasma treated using an Emitech K1050X plasma cleaner (Quorum Tech., UK) for 900s or 1800s and compared to untreated PEEK. Wettability, atomic force microscopy (AFM), and X-ray photoelectron spectroscopy (XPS) analyses were performed on the treated and untreated samples. Adhesion of 3 strains of *Staphylococcus aureus* (V8189-94, JAR and 8325-4) were measured to the materials in triplicate, with 9 samples of each surface in each replicate. Log phase bacterial cultures were adjusted to a density of $1x10^7$cfu/ml in PBS and incubated with the samples in a custom made adhesion chamber for 2.5h at ~37°C and 125rpm. After incubation, the bacterial suspension was replaced with fresh PBS and following sonication and vortex mixing viable counts of adherent bacteria on the samples were performed[2]. In addition, the adhesion of *S. aureus* JAR to oxygen plasma treated samples which had been exposed to 50% human blood plasma (fresh frozen plasma, Schweizerisches Rotes Kreuz GR, CH), centrifuged to remove any clots, in PBS were also assessed using the adhesion chamber. The samples were incubated in the chamber with 50% blood plasma for 1h (37°C,125rpm) before bacteria in PBS were added to give $1x10^7$ bacteria ml^{-1}. The experiment then proceeded as described above. The data were analysed using SPSS v.16.0. One-way ANOVA and *post hoc* LSD tests were used to compare Log_{10} transformed bacterial adhesion (n=3, Sig= P<0.05).

RESULTS: Plasma treatment of PEEK resulted in an decrease in hydrophobicity; an increase in atom% surface oxygen, as a result of an increase in oxygen functional groups; and a slight increase in surface roughness after 1800s treatment due to surface etching.

There was no significant effect on bacterial adhesion for the *S. aureus* strains in PBS (Fig 1a).

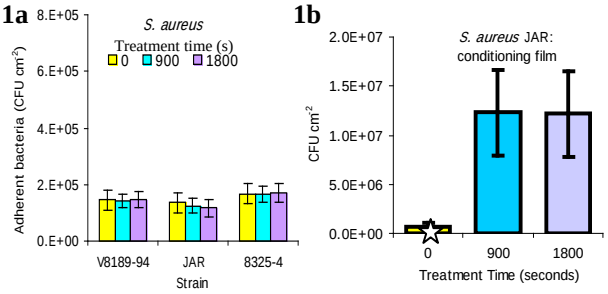

Fig. 1: Adhesion of S. aureus to the treated PEEK surfaces without PBS (1a) and Adhesion of S. aureus JAR to the treated and human plasma preconditioned PEEK surfaces, (1b) (n=3, ±s.e., Sig= P<0.05).

The presence of a conditioning film caused an increase in bacterial adhesion to the treated samples for the studied strain (Fig 1b). Plasma clotting was observed on the treated surfaces. The presence of clots provided an increased surface area which further enhanced bacterial adhesion.

DISCUSSION & CONCLUSIONS: The findings of this study show that plasma treatment may be a viable option for increasing osseointegration, without increasing the risk of peri-operative bacterial adhesion to PEEK in absence of a blood plasma conditioning film. The *in vitro* increase in bacterial adhesion to the treated materials in the presence of a conditioning film is due to a change brought about by the differential protein binding affinities of the treated samples and conformation of these bound proteins, and should be further investigated. This increase may be overcome by the positive effect previously reported for osteoblast cell adhesion and mineralisation due to the altered protein binding to the treated surfaces[1].

REFERENCES: [1]Poulsson, A.H.C. (2008) *Eur Cell Mater* 16: 47-47. [2]Altankov, G.; Groth, T. *J. Mater. Sci.* Mater. Med. 1994, 5, 732–737. [3]Miles, A.A. (1938) *J Hygiene* 38, 732-749.

ACKNOWLEDGEMENTS: Financial contribution and PEEK discs from Invibio Biomaterial Solutions, UK. Dr. Schulzki, RBSD SRK GR, for fresh frozen plasma.

Effect of Sintering Conditions on Physical Properties of TCP Ceramics

L. Galea, N. Doebelin, M. Bohner

RMS Foundation, Bettlach, Switzerland. laetitia.galea@rms-foundation.ch

INTRODUCTION: Many physical properties are known to affect the in vivo behavior of calcium phosphate bone graft substitutes. Some of the most important properties are the porosity, pore size and pore interconnection size. In recent years, there has been an increase of the interest devoted to the effect of grain size and microporosity. Unfortunately, it is difficult to modify one property at a time[1,2], and as a result, it is difficult to find a conclusive study. The aim of this study was to assess the possibility to use sintering as a way to modify one physical property at a time. A pre-sintering plateau was used to modify the density, grain size and specific surface area (SSA) of α-tricalcium phosphate (α-TCP) samples.

METHODS: An in-house produced α-TCP powder was milled 2h in a planetary mill with 10% fumaric acid and 2ml ethanol for 100g powder. The powder was then calcined for 12h at 400°C to remove the organic content. Cylindrical samples were prepared by uniaxial or isostatic pressing (both with P=200MPa). The uniaxially-pressed samples were pre-sintered 15h at $T_{plateau}$ = 600, 700, 800, 900, 1000 or 1150ºC and then sintered 1h at 1150ºC (Fig 1A). The isostatically-pressed samples were sintered 1h at T_{sint} = 900, 1000, 1100, 1200 or 1300ºC, with and without a pre-sintering plateau of 15h at 800ºC (Fig 1B). The heating and the cooling rates were 5°C/min and -1°C/min, respectively.

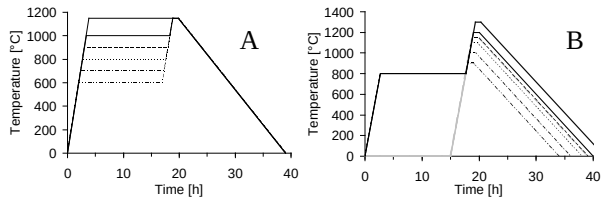

Fig. 1: Sintering for 1h A) at 1150°C with different pre-sintering temperatures. B) at different temperatures with and without pre-sintering.

After sintering, the relative density, ρ_{rel}, was measured by gravimetry, the SSA was measured by N_2 adsorption (BET model) and scanning electron microscopy observations of broken and thermally etched (900°C, 1h) surfaces were performed to assess the grain size. The crystalline composition was measured by X-ray diffraction. Result differences were evaluated with ANOVA. The significance level was set at p = 0.01.

RESULTS: $T_{plateau}$ had a strong effect on the samples ρ_{rel}: the value decreased from 84% at 600ºC to 81% at 800ºC and then increased to reach a value close to 88% above 1000ºC (Fig 2A). A pre-sintering had also an effect on the isostatically pressed samples: ρ_{rel} was roughly 3% lower at all T_{sint} (Fig. 2B). After an increase of ρ_{rel} between T_{sint}=900 and 1000°C, no significant change was observed at higher T_{sint} (Fig. 2B).

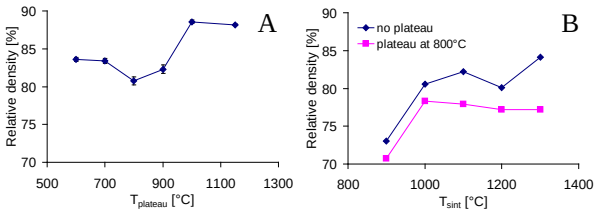

Fig. 2: The apparent density is affected by A) the pre-sintering temperature and B) the sintering temperature and a pre-sintering at 800°C.

An increase of T_{sint} increased the grain size (Fig. 3) and decreased the SSA, but these properties were not affected by a pre-sintering. All samples contained mainly α-TCP with up to 2wt-% β-TCP, except when a pre-sintering at 600°C was applied. In this case, the β-TCP fraction was about 15wt-%.

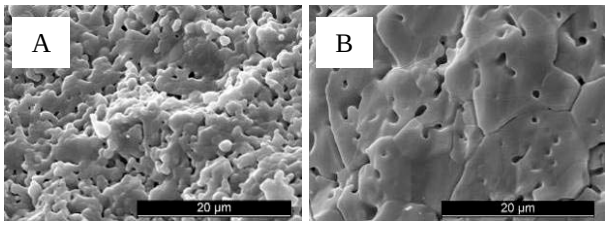

Fig. 3: 1h sintering at A) 1000°C and B) 1300°C.

DISCUSSION & CONCLUSIONS: The present results show that it is possible to vary the relative density without influencing the grain size, and inversely. In other words, a pre-sintering plateau and a change of sintering temperature could be used to produce samples with only one physical property varying at a time. This should help the design of in vivo studies aiming at determining the effect of physical properties (e.g. grain size, microporosity) on the biological response of calcium phosphate bone graft substitutes.

REFERENCES: [1]Habibovic P. et al., J Orthop Res 26:1363-70, 2008 [2]Yuan H. et al., J Biomed Mat Res A 78:139-147, 2006

Addition of strontium in a calcium carbonate - calcium phosphate mixed cement: release behaviour and effect on osteoprogenitor cells

S. Tadier[1], R. Bareille[2], R. Siadous[2], S. Cazalbou[1], O. Marsan[1], C. Rey[1], C. Combes[1]

[1] *Université de Toulouse, CIRIMAT, UPS-INPT-CNRS, ENSIACET, Toulouse, France.*
[2] *INSERM U1026 Bioingénierie Tissulaire, Université Bordeaux Segalen, Bordeaux, France.*

INTRODUCTION: Strontium has recently been proposed as an interesting additive in injectable biomaterials [1] for bone repair: minor constituent of bone, biocompatible, it is already used as a therapeutic agent in the treatment of bone pathologies (e.g. osteoporosis). In fact, at low doses it has a synergistic effect on osteoblast and osteoclast cells [2]. In addition, its introduction increases the radio-opacity of self-setting mineral bone cements, which is a prerequisite for their implantation using minimally invasive surgery techniques. However, high doses of strontium have been proved to be deleterious for the bone turnover. Therefore, the *in vitro* study of strontium release and biological activity of Sr-loaded cements appear to be important to understand their behaviour *in vivo*.

METHODS: The solid phase of the reference cement is composed of $CaCO_3$ vaterite and dicalcium phosphate dihydrate (DCPD), as described in details previously [3]. Strontium has been incorporated into these cements via two routes: as $SrCO_3$ in the solid phase or as $SrCl_2.6H_2O$ in the liquid phase. The *in-vitro* behaviour of these cements has been investigated: on one hand, cylinders of cements have been soaked for 3 weeks in a buffer solution at 37°C (0.1 M tris(hydroxymethyl)aminomethane at pH=7.4) to monitor the daily release rate of Ca^{2+} and Sr^{2+} ions and, on the other hand, disks of cements have been seeded with human osteoprogenitor cells to assess cell proliferation and differentiation. Cements were characterized by FTIR spectroscopy, Raman micro-spectroscopy, X-ray diffraction and SEM techniques before and after release tests and cell-culture.

RESULTS & DISCUSSION: Depending on the way strontium was introduced into the cement paste, set cements have different compositions and therefore different behaviours in solution.

When $SrCO_3$ is included in the solid phase it remains in the final cement which composition thus comprises carbonated apatite, vaterite and strontianite ($SrCO_3$) whereas when strontium chloride is introduced in the paste via the liquid phase no additional phase is detected compared to the reference cement and the formation of a partly Sr-substituted apatite was confirmed by XRD Rietveld refinement analysis. We demonstrate that vaterite dissolution was limited by a diffusion process during the *in vitro* test.

We show that, both in absence and in presence of osteoprogenitor cells, there is an initial Sr^{2+} and Ca^{2+} burst release during the first 48 hours; the level of release ions are higher for $SrCl_2$-loaded cements. Then, the release rate is slow and sustained for both cements which stimulates osteoblast cells and should promote early bone formation and contribute to the long-term success of bone substitution.

CONCLUSIONS: Strontium is a biocompatible radio-contrast agent that can be introduced either in the solid or in the liquid phase of $CaCO_3$-DCPD cements. *In vitro* tests show that there is an initial burst, followed by a sustained release leading to a beneficial effect of strontium on osteoblast cells especially when in contact with $SrCO_3$-loaded cements. Interestingly this study showed that we can optimize the sustained release of Sr^{2+}, the cement biodegradation and biological activity by controlling the route of introduction of strontium in the cement paste.

REFERENCES: [1] M. Bohner, U. Gbureck, J.E. Barralet, (2005) Biomaterials **26**:6423-6429. [2] P.J. Marie, P. Ammann, G. Boivin, C. Rey, (2001) Calcified Tissue International **69**:121-129. [3] C. Combes, B. Miao, R. Bareille, C. Rey, (2006) Biomaterials **27**:1945-1954.

Alginate-PEG Hybrid Microspheres for Biomedical Applications

R. Mahou[1], C. Gonelle[2], G. Parnaud[2], F. Schmitt[3], G. Kollárková[4], L. Juillerat-Jeanneret[3], I. Lacík[4], C. Wandrey[1]

[1]EPF Lausanne, Switzerland, [2]University of Geneva, Switzerland, [3]CHUV, Lausanne, Switzerland, [4]Polymer Institute of the Slovak Academy of Sciences, Bratislava, Slovakia

INTRODUCTION: Hydrogel microspheres with sodium alginate (Na-alg) as major component are among the most suitable materials for cell immobilization. Ionotropic gelation of Na-alg in presence of divalent cations yields such hydrogels. However, they suffer from mechanical stability deficiency, limited durability, and permeability drawbacks. Frequently used reinforcement with polycations requires multi-step processes and can have a negative impact on the biocompatibility. Our approach combines ionotropic gelation of Na-alg and covalent cross-linking of PEG derivatives in one step and yields alginate-PEG hybrid microspheres (Alg-PEG-M) convertible into PEG beads (PEG-M) [1].

METHODS: Alg-PEG-M and PEG-M were prepared at 37°C under physiological conditions using a coaxial airflow droplet generator (Fig.1).

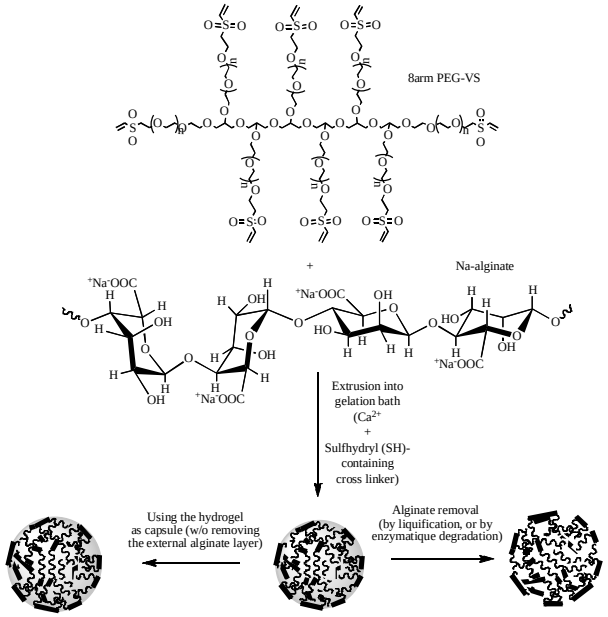

***Fig. 1**: Formation process to obtained spherical and uniform Alg-PEG-M (left) and PEG-M (right).*

RESULTS AND DISSCUSSION: The precursor quality and concentration govern the mechanical resistance. Dissolution of Ca-alg slightly raises the mechanical resistance to compression (Fig.2). The permeability can be tailored by adequate choice of the arm length of PEG-VS. The MWCO was tuneable in a range of 70 to 150 kg/mol.

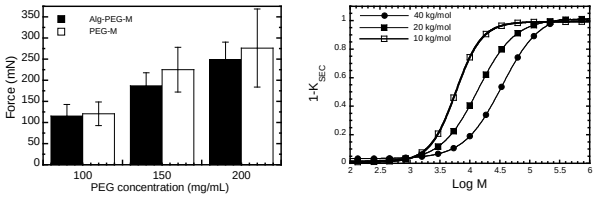

***Fig. 2**: Resistance to 80% compression for three PEG-VS concentrations before and after Ca-alg liquefaction. (left), MWCO for three PEG-VS types (right).*

Cell toxicity of Alg-PEG-M assessed for EC219 rat endothelial cells, ECp23 murine endothelial cells, and RAW264.7 murine macrophages did not reveal cytotoxic effects (examples in Fig.3).

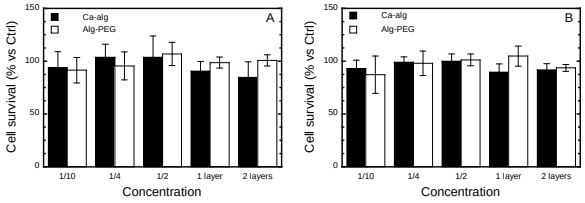

***Fig.3**. Cell survival. EC219 rat endothelial cells (A) ECp23 murine endothelial cells (B), 24 h incubation.*

The immune response upon intraperitoneal implantation into mice was comparable to the control and pure Ca-alg microbeads (Fig.4).

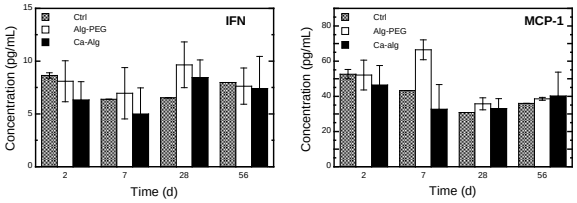

***Fig. 4**: No significant increase of cytokines in the mice serum up to 8 weeks, (selected results).*

Encapsulated human islets continued insulin secretion upon stimulation.

CONCLUSIONS: Combining ionotropic gelation and chemical cross-linking in a one-step process yields Alg-PEG-M with well-controllable physical properties. Significant toxic effects were observed neither *in vivo* nor *in vitro*.

REFERENCES: R. Mahou, C. Wandrey (2010) *Macromolecules* 43(3). 1371-1378.

ACKNOWLEDGEMENTS: We thank the SNF for supporting this research, Grants 205321-116397/1205320-130572/1.

Electrochemical Impedance technique in understanding diagnostic and prediction of oral dental diseases

V. Penta, M. Dilea, C. Pirvu, D. Demetrescu [1]

INTRODUCTION: Electrochemical impedance spectroscopy (EIS) is a very useful laboratory procedure[1] broadly applied in our days especially in characterizing electrode processes and complex interfaces. The aim of this paper is focussed on a novel approach in using this technique related to the possibility of evaluation oral health measuring EIS parameters of various teeth[2] and proposing equivalent circuits fitting EIS data. Despite the fact that teeth are ceramic materials and perfect insulators while dry, if placed into a solution that resembles the physiological fluid EIS measurement can be obtained. The study is divided into three kinds of EIS applications in oral health as following; the first part is in relation with the effect of EDTA combined with urea peroxide in teeth root canal therapy. The second and third parts were concerned with demineralization process from temporary teeth gathered from different area of Romania having high level of pollution[3] (which contain heavy metals) and from cracked teeth respectively.

METHODS: Extracted children teeth were prepared according to a protocol as following:

- samples surface characterization involves microscopic analysis in order to detect any lesions or micro-cracks which were perform with an Zeiss Scope.A1 optical microscope and contact angle measurements to quantify the wettability. Wetting was evaluated by using a Contact Angle Meter –KSV Instruments CAM 100. The EIS analysis was carried out using an Autolab PGSTAT 302N potentiostat with NOVA 1.6 software.

In order to prove the effectiveness of EDTA with urea peroxide a number of 20 human extracted teeth on which we performed root canal therapy using Pro-taper file system. The exact method is as follows. The teeth have had root canal therapy after the radiological establishment of the working length. A copious irrigation with NaOCl 5% was done. After sealing the apex with composite resin we placed a platinum rod inside each root. The EIS cell comprised a reference Ag/AgCl electrode, a platinum counter electrode, a working electrode and a cylindrical chamber. As a working electrode, teeth samples (whole tooth and dentin) were used.

EIS of the specimens were measured at a series of immersed interval. Data obtained is expressed graphically in a Nyquist plot.

RESULTS: In fig. 1 as an example of the EIS use data is presented Nyquist plot for teeth root canal treated and untreated with EDTA.

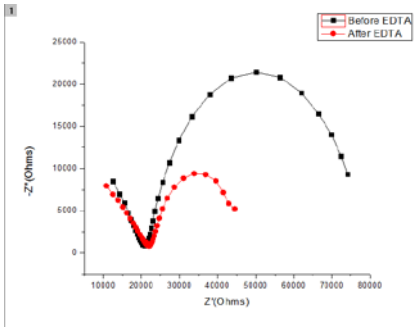

Figure. 1 Nyquist plot for teeth root canal treated (red) and untreated (black) with EDTA.

The figure is an expression of teeth behaviour according to the decrease of resistance parameters Rd, which is the resistance of the sample layer and Rct, which is the charge transfer associated with the penetration of electrolyte in teeth decreased with increasing of demineralization. Same kind of significant decrease in resistance values due to differences in demineralization level can be seen in the case of teeth provided from areas with different pollution. Hydrophilic /hydrophobic balance and ICP-Ms measurements as complementary techniques are supports in understanding the demineralization mechanism

DISCUSSION & CONCLUSIONS: This investigation suggests that the EIS technique is efficient in monitoring the demineralization process of teeth and understanding their surface structural changes which may induce disease. It is a possible method of future diagnostic in the Cracked Tooth Syndrome for which there are rather scarce diagnostic possibilities.

REFERENCES: [1] A Lasia, Electrochemical impedance spectroscopy and its applications in Modern aspects of electrochemistry Edts Kluwer, Plenum Publisher. B.E. Conway, J Bokris, and R White(1999) Kluwer Publisher vol32pp 143-248 [2]Aziza HE, Alec SH, Girish MK..Journal of Dentistry 2004;32:547–54. [3]I.Demetrescu D.Ionita Molecular Crystal & Liquid Cryst., 2010 Vol. 523 pp. 73–81

ACKNOWLEDGEMENTS: This template was modified with kind permission from European cells and Materials Conferences (http://www.ao-asif.ch/ari/meetings.shtml).

Near-infrared light curable composites for advanced dental applications

A.Stepuk, D.Mohn, W.J.Stark

ETH Zurich, Institute for Chemical and Bioengineering, Switzerland

INTRODUCTION: Light-curable dental polymers (resins) are commonly used in restorative surgery, prosthodontics and surgical procedures. Despite the fact of wide application, there are clinical problems due to limitations of blue light penetration: application is restricted to defects exposed to the light source; layered filling of defect is required [1]. Enhanced transmittance of near-infrared light (NIR) through the tissue could allow polymerization in complex shaped defects. The prerequisite 450 nm blue light to polymerize dental resins could be achieved by filler particles, which absorb the incident NIR irradiation and convert it into visible light. The process is known as upconversion (UC). The Figure 1 demonstrates both procedures: applying UC and traditional.

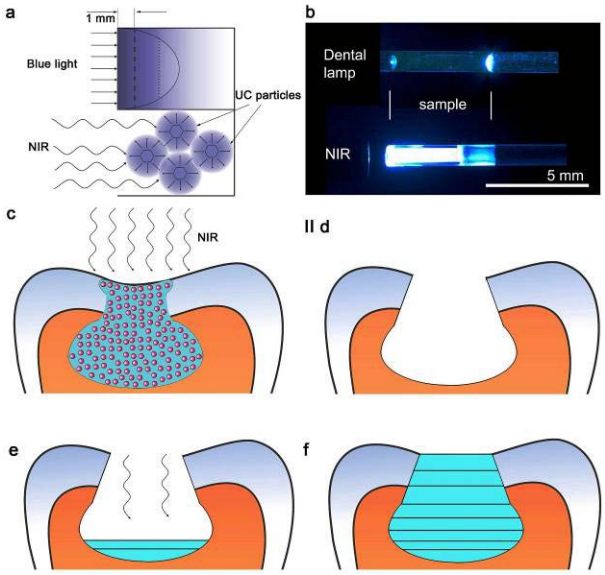

Fig. 1: Approach scheme. I Treatment with composite: (a) light curing of the polymer vs. blue light emission by upconversion of $NaYF_4$:Yb,Tm particles; (b)photograph of the blue light emission/propagation for pure polymer and composite doped with UC phosphors; (c) one-step filling and curing with NIR light; II Current treatment: (d) preparation and cleaning of a cavity; (e) layer-by-layer filling followed by curing with blue light; (f) final filling consisting of several layers

This study represents an alternative approach in curing dental resins by NIR source.

METHODS: Blue-light emitting hexagonal UC particles ($NaYF_4$: Yb,Tm) were fabricated by solid state synthesis [2]. Absolute luminescence of microcrystalline UC particles was examined in frame of their excitation rates. Dental resins were doped with UC phosphors in different ratios (0/100, 10/90 or 20/80) and cured by a NIR laser source ($\lambda = 980 \pm 5$ nm), from 30 sec till 10 min. The degree of conversion (DC) of cured composites was determined from the ratio of absorbance intensities of C=C and C•••C bonds before and after curing. Dentine and enamel cross-sections (0.5 mm thick) were analysed with respect to the radiation transmission and used as a closed cavity model for application of dental resins.

The incorporation of UC phosphors into the polymeric matrix led to a uniform hardening in bulk. Composite samples of 5 mm thickness were cured two times faster than pure polymer cured by blue light. The enhanced penetration of NIR light was confirmed by calculating the optical penetration depth and by curing the samples through enamel/dentine obstacles. The NIR and blue light cured samples showed a monomer conversion of 40 %.

RESULTS: Embedding UC phosphor particles into dental resin allowed curing with NIR laser irradiation, which can be an attractive treatment of closed defects, not accessible to direct light exposure [3]. Optical analysis of dentine and enamel demonstrated transmittance surge in 800÷1200 nm diapason. Fast curing, one-layer application and high monomer conversion rates could provide a new valuable and competitive dental restorative material.

REFERENCES: [1] R.G. Craig, *Restorative Dental Materials*. Mosby: St. Louis, 1997. [2] K.W. Kramer, et al., *Hexagonal sodium yttrium fluoride based green and blue emitting upconversion phosphors. Chemistry of Materials*, 2004. 16(7): p. 1244-1251 [3] A. Stepuk et al., *in preparation*, 2011.

Smart Root Canal Fillings for Advanced Endodontic Applications

D. Mohn[1], M. Marending[2], M. Zehnder[2], W.J. Stark[1]

[1] *Department of Chemistry and Applied Biosciences, ETH Zurich, 8093 Zurich, Switzerland.*
[2] *Department of Preventive Dentistry, Periodontology, and Cariology, University of Zurich, Center of Dental Medicine, 8032 Zurich, Switzerland.*

INTRODUCTION: To fill a root canal the dentist needs 2 materials: an inert core (Gutta-percha, GP) and a sealer that provides canal wall adaptation and a hermetic seal[1]. The core is generally bioinert, while the sealer often causes tissue irritation. Instead of using the conventional approach it would be advantageous to use just one smart material that provides both properties[2] and does not irritate tissues. Novel bioactive root canal filling materials were tested *ex vivo* in single-rooted human teeth regarding their canal wall adherence without the use of a sealer for advanced adaptation and a simplified handling procedure.

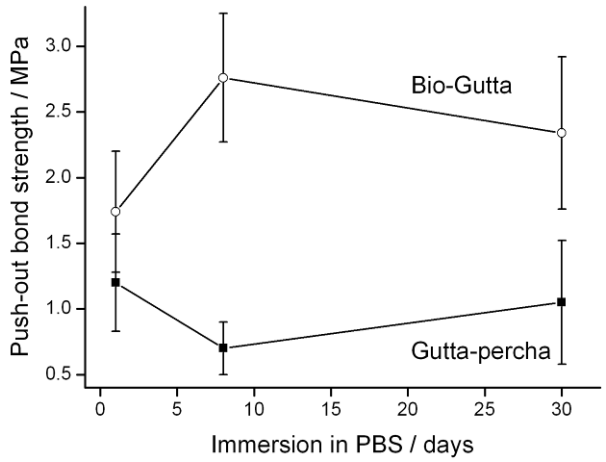

Fig. 1: Push-out test values of materials over time when filled roots were immersed in PBS.

METHODS: Conventional GP (70% ZnO and 30% polyisoprene) and a so-called Bio-Gutta (45% ZnO, 30% polyisoprene and 25% bioactive glass) were prepared on a roller mill. Root canals of 66 extracted single-rooted teeth were instrumented and rinsed with 1% NaOCl followed by 17% EDTA. Thirty-three roots were filled with GP, 33 with Bio-Gutta. Warm vertical compaction was applied. Specimens were immersed in phosphate-buffered saline for up to 30 days. Two slices of 1.5 mm each were cut from each root perpendicular to its long axis in the middle third to perform push-out tests using an universal testing machine. Root fillings were loaded with a 0.8-mm cylindrical plunger at 0.5 mm/min cross-head speed. Data were compared between groups using one-way ANOVA/Bonferroni, alpha = 0.05. Furthermore, test materials were examined for their radiopacity.

RESULTS: Both materials under investigation had similar initial push-out bond strength ($p > 0.05$). The adherence of Bio-Gutta increased from day 1 to 7 (Fig. 1) and was significantly better than that of conventional GP at 7 and 30 days ($p < 0.05$). Test materials showed similar radiopacity; 5.4 mm and 5.7 mm aluminium for Bio-Gutta and GP, respectively.

DISCUSSION & CONCLUSIONS: Conventional GP exhibited inert properties, which contrasted with those of the bioactive root filling material. Apatite formation at the interface to the root canal wall as well as moisture expansion might be responsible for the increasing adherence of Bio-Gutta between day 1 and day 7 (Fig. 2). Future experiments should investigate what happens at the interface between dentin and this new material.

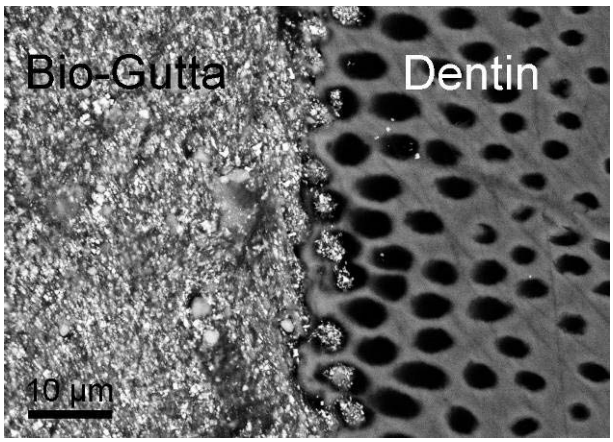

Fig. 2: SEM image showing the smooth canal wall adaptation after 1 day immersion of the root-filled tooth in PBS.

REFERENCES: [1] M. Torabinejad and R.E. Walton (2009) *Endodontics, Principles and Practice*, Saunders, Elsevier. [2]D. Mohn, C. Bruhin, N.A. Luechinger, W.J. Stark, T. Imfeld, M. Zehnder (2010) *Int Endo J* **43**:1037-46.

ACKNOWLEDGEMENTS: Financial support by the Department of Preventive Dentistry and Oral Epidemiology, University Zurich is kindly acknowledged.

Sustained N-Methyl Pyrrolidone Delivery with In Situ Forming Implants for Use as a Guided Bone Regeneration Membrane

L.S. Karfeld-Sulzer[1], J.C. Leroux [2], F.E. Weber[1]

[1] *University Hospital Zurich, Zurich, Switzerland.* [2] *ETH Zurich, Zurich, Switzerland.*

INTRODUCTION: The success of dental implants requires sufficient alveolar bone density and quality. Guided bone regeneration (GBR) membranes have been designed to exclude soft tissue ingrowth through a physical barrier, enabling infiltration of slower-growing bone cells. An optimal environment should prevent formation of soft tissues, but also encourage bone augmentation through appropriate biochemical cues. Bone morphogenetic proteins (BMPs) are critical in bone formation and their importance has been affirmed with GBR [1]. However, effective concentrations are very high, which constitutes an expensive treatment with potential negative side effects [2]. Previously, we have demonstrated that N-methyl pyrrolidone (NMP) is a potent enhancer of BMP activity that can increase bone regeneration markers without high BMP concentrations [3]. For this therapy to be clinically effective, we aim to deliver NMP in a sustained manner. Since NMP is a small, water- and organo-miscible molecule, many traditional drug delivery strategies are not sufficient. In the present work, we have employed polyesters as in situ-forming implants (ISFI) for sustained NMP delivery.

METHODS: All polylactide and poly(lactide-co-glycolide) polymers were obtained from Boehringer Ingelheim. Polymers were dissolved overnight at 40 wt% in NMP at 37°C. Release studies were performed by injecting the dissolved polymer into a metal mesh basket and immediately immersing it into phosphate buffered saline. Samples were maintained at 37°C on a shaker. Periodically, an aliquot of release buffer was removed and analyzed using liquid chromatography-mass spectrometry. NMP concentration was quantified using the area under the curve of the UV signal at 210 nm.

Initial polymer molecular weights and polymer degradation were analyzed with gel permeation chromatography with refractive index detection and polyethylene glycol standards for molecular weight calibration. The degradation study was performed similarly to the release study except that implants were removed at specified time points, rinsed with deionized water, and frozen at -80°C until analysis.

RESULTS: The release profiles of NMP from polymer implants with different molecular weights (MW) and lactide to glycolide ratios (L:G) were studied. All of the formulations had some amount of initial burst release, but it was limited to less than 20% after 8 hours for the lower MW polymers. A comparison of different MW polymers with L:G = 50:50, shows that the lowest MW of 14.5 kDa was initially lower than the 22.8 kDa polymer. However, after 3 days, the release from the 14.5 kDa polymer surpassed the 22.8 kDa polymer, which may be attributed to polymer degradation. Degradation studies show an immediate linear decrease in average molecular weight. L:G ratio also impacts release characteristics. Release experiments with polymers of similar low MW demonstrated that the L:G = 100:0 polymer has a significantly higher burst release. The L:G = 75:25 polymer showed both the least burst and the longest period of release, with 17% and 81% release after 24 hours and 21 days, respectively.

DISCUSSION & CONCLUSIONS: Previous unpublished studies with other delivery systems were insufficient to retain NMP for more than 2 days. By exploring different polymer MW and L:G, we have found that ISFI are able to retain NMP for at least 21 days. This extended release would enable the BMP-enhancing effects of NMP to be realized for a greater period. When the water-insoluble polymers of the ISFI are exposed to water, they undergo a phase transition and a membrane is formed on the implant [4]. The rates of the simultaneous water diffusion into the implant and NMP diffusion out of the implant are dependent on the polymer properties and rate of phase transition. This ISFI system is potentially viable for sustained NMP delivery.

REFERENCES: [1] U.M. Wikesjo, M. Qahash, Y.H. Huang, et al (2009) *Orthod Craniofac Res* **12**:263-70. [2] W. Zhu, J. Kim, C. Cheng, et al (2006) *Bone* **39**:61-71. [3] B.S. Miguel, C. Ghayor, M. Ehrbar, et al (2009) *Tissue Eng Part A* **15**:2955-63. [4] A.J. McHugh (2005) *J Control Release* **109**:211-21.

Bone augmentation for inserting oral implants

B. Ilgenstein, H. Deyhle, and B. Müller

Biomaterials Science Center, University of Basel, Switzerland.

INTRODUCTION: Oral implants have been a vital part of reconstructive dentistry. The insertion of dental implants is a well-established procedure performed in many offices. Nevertheless, the successful osseointegration of dental implants depends on the proper implant surface and the bone-offer. Frequently, local bone defects result from tooth extraction or pathological absorption so that the insertion of an implant is impossible. In these cases, bone augmentation is required before implantation. The reconstruction with autologous bone, which is still the gold standard, is often difficult for surgeon and patient, as it has to be taken from intra- or extra-oral donor sites. Therefore, bone substitutes are playing a more and more important role in augmentation surgery. Their composition and microstructure is responsible for the osseo-integration and osseo-conduction of the implants. In this communication, we evaluate bone augmentation materials of established suppliers.

MATERIALS & METHODS: Synchrotron radiation-based micro computed tomography (SRμCT) has been developed to a complementary method to histological sectioning. Because bone augmentation treatments using artificial calcium phosphate phases need months, one aims to identify the most effective biomaterials for bone augmentation. Here, we compare a set of specimens from patients, who obtained comparable treatments with different ceramic biomaterials. Before implant insertion, the oral surgeon prepares the hole for the implant by means of a hollow drill, which enables storing the specimens for detailed SRμCT-measurements and -analysis. One typical bone augmentation material is easy-graft™ (Degradable Solutions AG, Schlieren, Switzerland). Such a specimen has been harvested after about six months and embedded for SRμCT measurements at the beamline W2 (HASYLAB at DESY, Hamburg, Germany), which is operated by the Helmholtz Centre Geesthacht, Germany. Using a photon energy of 25 keV, 900 radiographs between 0 and 180° were recorded. The pixel size after two-fold binning corresponds to 4.3 μm. The reconstruction by means of the filtered back-projection algorithm provided a tomography with a size of 1526 × 1526 × 835 voxels. VG Studio Max 2.1 (Volume Graphics, Heidelberg, Germany) served for the visualization of the virtual slices.

RESULTS: Fig. 1 shows three virtual cuts perpendicular to each another through the tomogram of the PMMA-embedded easy-graft™ biopsy. The bright spherically shaped features belong to the augmentation material and are not yet fully absorbed. The gray-coloured parts are newly formed bony tissues with characteristic morphologies.

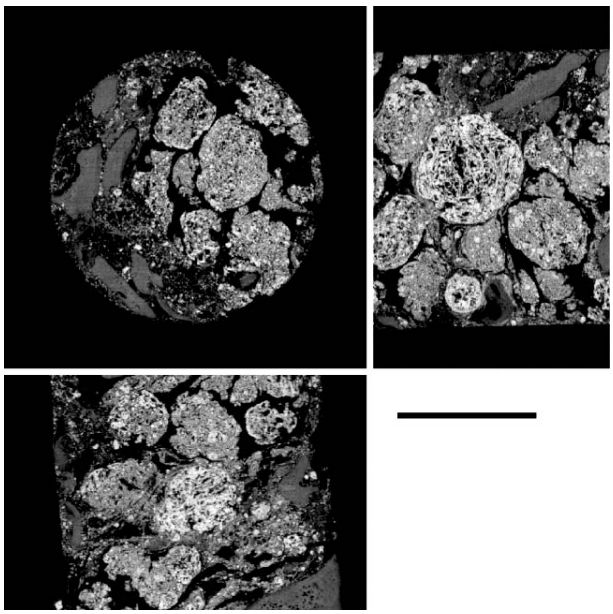

Fig. 1: Three orthogonal virtual cuts through the tomogram of a biopsy extracted from human jaw six months after augmentation material placement. The bar corresponds to 1 mm.

DISCUSSION & CONCLUSIONS: SRμCT provides three-dimensional data that allow for the quantification of newly formed bone and absorbed augmentation material. Furthermore, one can determine the contact areas between bone and biomaterial to characterize the established materials for bone augmentation. The present study, which includes different research teams, finally aims to identify bone augmentation materials with optimized performance.

ACKNOWLEDGEMENTS: The support of Dr. Felix Beckmann (Helmholtz Centre Geesthacht) is gratefully acknowledged. The authors thank HASYLAB for providing beamtime within approved proposals.

Adsorption of an enamel matrix derivative (EMD) to a bovine derived bone grafting material in the presence of human blood

Richard J. Miron[1], Dieter Bosshardt[1,2], Beat Haenni[3], Daniel Buser[2], Anton Sculean[1]

[1]Deparment of Periodontology, [2]Deparment of Oral Surgery and Stomatology, School of Dental Medicine, University of Bern, Freiburgstrasse 7, 3010 Bern, Switzerland
[3]Institute of Anatomy, University of Bern, Baltzerstrasse 2, 3000, Bern, Switzerland

Abstract

Background: Protein adsorption to biomaterials is a crucial interaction that influences downstream cellular pathways such as cell adhesion, proliferation and differentiation. Recently, the use of bone grafting materials in combination with various biologic active agents such as growth factors or an enamel matrix derivative (EMD) has been shown to significantly enhance the clinical outcomes following regenerative periodontal surgery. At the present time, it is unknown to what extent the bleeding during regenerative surgery may compete with the adsorption of proteins to the surface of bone grafting materials.

Aim: To evaluate the effect of blood interactions on EMD adsorption to bone grafting particles.

Material and Methods: Natural Bone Mineral (NBM) particles were coated with EMD and human blood samples were either added prior to or after EMD coating for varying periods of time. Particles were analyzed for protein adsorption via fluorescent imaging for anti-EMD antibody labeling. Paraffin and LR White sections were also analyzed for anti-EMD protein binding to the interior of NBM particles. Scanning electron microscopy was used to visualize protein interactions on the surfaces of NBM particles.

Results: The interaction between blood and EMD adsorption was significantly affected based on the stage at which blood contacted NBM particles. EMD adsorption was significantly decreased when NBM particles were pre-coated with blood followed by EMD. SEM analysis of EMD coated particles revealed protein deposition on the surfaces of NBM particles. Blood treated particles were densely covered by erythrocytes and blood plasma proteins preventing future adsorption of EMD.

Conclusion: The present findings indicate that: a) the presence of blood negatively affects the adsorption of EMD to NBM particles and b) blood interactions with bone grafting particles during regenerative periodontal surgeries should be minimized in order to allow better EMD adsorption.

Keywords: Enamel matrix derivative (EMD), Emdogain, natural bone mineral, blood proteins, protein adsorption, bone grafting materials

Structural anisotropies of PEEK foils revealed by optical dichroism and X-ray scattering methods

J.Althaus[1,2], H.Deyhle[1,2], O.Bunk[2], and B.Müller[1]

[1]*Biomaterials Science Center, University of Basel, Switzerland.*
[2]*Paul Scherrer Institute, Villigen, Switzerland.*

INTRODUCTION: During the last three decades, poly-aryletherketones and especially poly-etheretherketone (PEEK) have been increasingly employed as biomaterials for trauma, orthopaedic, and spinal implants.[1] PEEK is biocompatible, inert and exerts excellent mechanical properties compared to other polymer materials. As its chemical nature suggests structural anisotropy, we investigated PEEK foils using optical and X-ray scattering methods.

METHODS: Commercially available amorphous and semi-crystalline APTIV™ PEEK foils (Series 2000 and 1000, Victrex Europa GmbH, Hofheim, Germany) were marked for direction of rolling. Hot embossing was done with a HEX03 press (JENOPTIK Mikrotechnik GmbH, Germany) at 160 °C and 100 kN. For the optical transmission measurements, the foils were mounted on a 360° rotation table and measured at different wave-lengths with a spectrophotometer (Perkin Elmer, Germany). The small- and wide-angle X-ray scattering (SAXS/WAXS) data were recorded at the cSAXS beamline of the Swiss Light Source (Paul Scherrer Institute, Villigen, Switzerland) in scanning setup.[2] Foils were mounted on an aluminium holder for line scan acquisition.

RESULTS: Absorbance scans parallel and perpendicular to the direction of rolling reveal that semi-crystalline and hot-embossed amorphous PEEK foils are anisotropic contrary to amorphous untreated foils. Around 540 nm, the anisotropy reaches a maximum. Measuring the transmission at 540 nm as a function of rotation angle results in a sine with 3.9% amplitude, suggesting a linear orientation in the foil. The transmission is minimal in rolling direction.

SAXS of the embossed 50 µm-thin PEEK foils also shows the anisotropy revealed in the optical measurements (see Fig. 1). The spot intensity increases with foil thickness from 12 µm via 25 µm to 50 µm. While the semi-crystalline foils also exhibit the anisotropy, the amorphous untreated foils are isotropic. The anisotropy detected in SAXS corresponds to a feature size of about 140 Å. Such a long-range order was already described.[3]

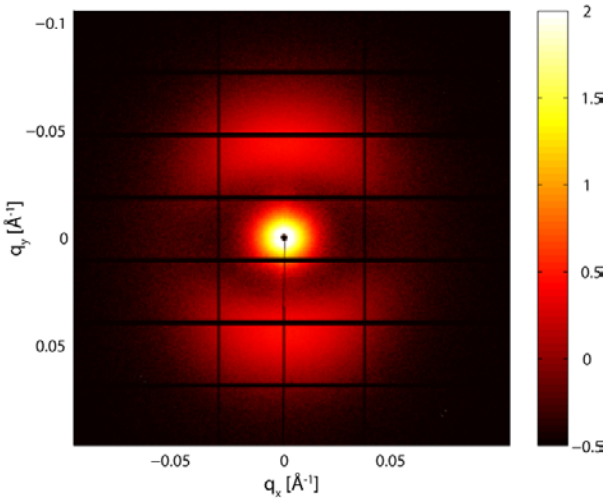

Fig. 1: SAXS pattern of 50 µm-thin embossed PEEK foil, acquired with 11.2 keV photons using 1 s exposure time, averaged over 60 frames.

The unit cell of solution crystallized PEEK is described as orthorhombic with a = 7.75 Å, b = 5.89 Å, and c = 9.88 Å.[4] The WAXS measurements exhibited peaks at q-values of 0.79 Å^{-1} and 1.06 Å^{-1}, corresponding to 7.9 Å and 5.9 Å, respectively, which is in reasonable agreement with the a- and b-values.

DISCUSSION & CONCLUSIONS: Hot embossing of amorphous PEEK foils above glass transition temperature results in anisotropic properties in rolling direction. The direction and the extent of anisotropy in crystalline PEEK foils can be quantified by rather simple optical transmission measurements. SAXS scans identify the equivalent orientation with nanostructures of approximately 14 nm-long units. The data should allow building a structural model to describe this long-range order in PEEK foils.

REFERENCES: [1]S.M. Kurtz and J.N. Devine (2007) *Biomaterials* **28**:4845-69. [2]O. Bunk et al (2009*) New J Phys* **11**:123016. [3]D.J Blundell and B.N. Osborn (1983) *Polymer* **24**: 953-958. [4]A.J. Lovinger and D.D. Davis (1986), *Macromolecules* **19**:1861-1867.

Crystallographic phases of NiTi scaffolds fabricated by selective laser melting

T. Bormann[1,2], R. Schumacher[1], B. Müller[2], M. de Wild[1]

[1]School of Life Sciences, University of Applied Sciences Northwestern Switzerland, Muttenz, Switzerland. [2]Biomaterials Science Center, University of Basel, Basel, Switzerland.

INTRODUCTION: FDA-approved NiTi[1] belongs to the shape memory alloys (SMA) which exhibit superelasticity and the shape memory effect. The reason behind is a reversible phase transition from the low-temperature martensite to the high-temperature austenite. As the shape memory effects and therefore the physiological reactions are intrinsically linked to the crystal structure, we have used x-ray diffraction (XRD) to characterise the specimens. In this study, we used the additive manufacturing technique of selective laser melting (SLM) to fabricate free-form NiTi parts (Fig. 1) with shape memory properties and different phase transition temperatures.[2]

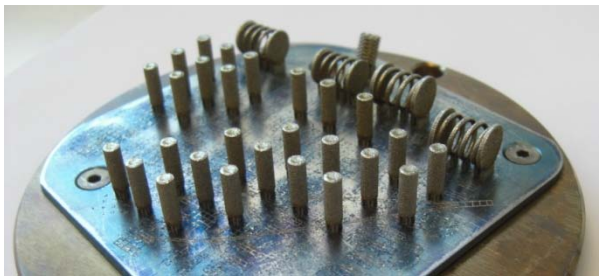

Fig. 1: NiTi samples produced by SLM.

MATERIALS & METHODS: NiTi-specimens were manufactured from NiTi-powder (MEMRY GmbH, Weil am Rhein, Germany) using the SLM Realizer 100 (SLM-Solutions, Lübeck, Germany). Different energy densities within the fabrication process as well as subsequent heat treatments at 800 °C were applied to generate specimens with different phase transition temperatures. Differential scanning calorimetry (DSC) and x-ray diffraction (XRD) measurements were accomplished at the NiTi-powder and two samples whose phase transition temperatures lie beneath and above room temperature, respectively. The austenite peak temperature A_p of Sample 1 was -3 °C whereas A_p of Sample 2 corresponded to 50 °C. XRD measurements were done at room temperature using CoKα radiation.

RESULTS & DISCUSSION: As expected, the preliminary XRD measurements reveal differences in the spectra depending on the measured phase transition temperatures. The peaks of Sample 1 mainly relate to austenite with a cubic crystal lattice (see Fig. 2). This is not surprising, since the phase transition takes place below room temperature, i.e. the material is in its high-temperature austenitic phase at room temperature. For Sample 2, whose A_p lies above room temperature, mainly martensite phase with a monoclinic crystal lattice is expected. The spectrum, however, not only shows martensite but also austenite peaks, as illustrated in Fig. 2. That means in Sample 2 both phases are in coexistence. The DSC investigation on Sample 2 reveals that the starting point of the phase transition lies already at 26 °C. A reason for the austenite phase in Sample 2 could therefore be a start of phase transition due to a slight increase in the sample surrounding temperature, caused e.g. by the XRD investigations itself.

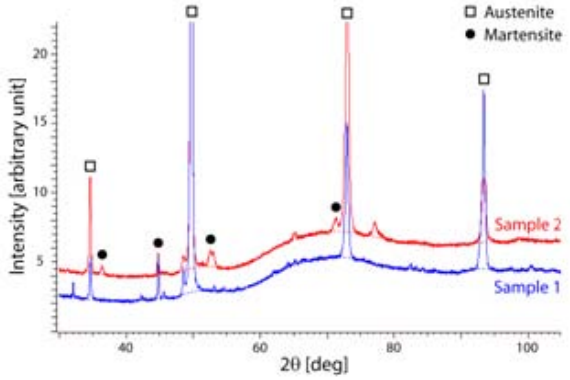

Fig. 2: XRD-spectra of two SLM samples with different process histories.

CONCLUSION: In this preliminary XRD study, we find differences in the crystallographic structure of our SLM samples, which have been produced by different processing procedures. Quantification of the two phases and correlation with the ability for the shape memory will contribute to our final aim, the realization of complex-shaped NiTi-implants with advanced performance.

REFERENCES: [1]ASTM International, F 2063 - 05. [2]T. Bormann *et al.*, Proc. of SPIE **7804**:78041.

ACKNOWLEDGEMENTS: The multi-disciplinary team gratefully acknowledges the financial support of the Swiss National Science Foundation within the program NRP 62 ‘Smart Materials‘.

Luminex®: A New Tool to Investigate the Cytokine Profile Secreted by Human Macrophages after Contact with Biomaterials - Example of Tricalcium Phosphate

D.S.Tavares[1,2], T.H.Gasparoto[3], D.H.Yassuda-Mattos[1], N.M.F.Costa [1], P.A.L.Lima[2,5], M.S.Sader[1], G.G.Alves[4], A.P.Campanelli[3], G.A.Soares[1], J.M.Granjeiro[4], K.Anselme[2]

[1]Materials and Metallurgical Engineering Department, Federal University of Rio de Janeiro, Rio de Janeiro, Brazil, [2]Materials Science Institute of Mulhouse, Haute-Alsace University, Mulhouse, France, [3] Faculty of Dentistry, University of São Paulo, Bauru, Brazil, [4] Cell and Molecullar Biology Department, Federal Fluminense University, Niterói, Brazil, [5] Materials Department, Federal University of Sergipe, São Cristóvão, Brazil

INTRODUCTION: Tricalcium phosphate (TCP) is one of the most used biomaterial as bone graft, due to its similar composition to the mineral bone phase. Likewise, magnesium ions can be incorporated in the crystal lattice of tricalcium phosphate (β-TCMP) to improve their biological activity, since it is the most abundant ion in bone tissue during osteogenesis[1]. The implantation of a biomaterial involves tissue trauma, which induces an inflammatory response mainly mediated by macrophages. The Luminex® xMAP technology is a useful tool to investigate several molecules in only one sample[2]. The aim of this work was to produce dense granular β-TCP and β-TCMP in order to investigate the cytokine profile secreted by human macrophages after contact with the materials extracts *in vitro* through Luminex®.

METHODS: Mg-substituted calcium deficient apatite (the transformation to TCP occurs after sintering) containing 0.15mol of Mg was synthesized as previously described[3]. A solution containing 1.3M $Ca(OH)_2$ and 0.17M $MgCl_2.6H_2O$ was dropped simultaneously with a 0.17M H_3PO_4 solution into water over 3h (39°C, pH 9). The powders of both materials (β-TCMP and β-TCP, MERCK, Germany) were pressed, sintered at 1150°C for 4h and crushed to obtain granules in the range of 250-500μm. The materials were characterized through X-ray diffraction (XRD) and infrared spectroscopy (FTIR). Samples were extracted in culture medium (100mg/ml, granules/RPMI free of FBS) at 37°C for 24h according to ISO 10993-12 and 10993-5. Through the Luminex® assay, 16 cytokines (G-CSF; GM-CSF; IFN-γ; IL-1β; IL-6; IL-8; MCP-1; MCP-3; MIP-1α; MIP-1β; MIP-3α; PDGF-bb; TNF-α; VEGF; IL-1ra; IL-10) were measured from supernatants of activated (10ng/ml LPS) and non-activated macrophages (isolated from human peripheral blood) cultivated with and without (control) the biomaterial's extracts after 24, 48 and 72h. The test was performed in triplicate.

RESULTS: The diffraction pattern of the sintered powders showed the peaks of β-TCMP and β-TCP. FTIR spectroscopy showed bands characteristic of TCP. Regarding the inactivated macrophage assay, when comparing the control and the macrophages cultivated with the biomaterial´s extracts, it was verified an increase in the pro-inflammatory cytokines. However, the results of the activated assay show an opposite effect, a decrease in the pro-inflammatory cytokines production. It was also verified that the pro-inflammatory cytokines production was elevated after macrophages activation, when comparing the controls and reduced, when comparing the biomaterials.

DISCUSSION & CONCLUSIONS: The fact that the pro-inflammatory cytokines production was smaller after macrophages activation when comparing the biomaterials suggests an inhibition of macrophage response to pathogens in their presence. For instance, when a biomaterial is implanted in the oral cavity, an environment full of bacteria, the macrophage response could be reduced. In a general way, there was not a significant difference of the cytokine profile induced between the biomaterials, even after macrophage activation. This suggests that magnesium addition to TCP might not promote substantially different immune responses in vivo. This study also demonstrates the efficiency and utility of Luminex® for simultaneous and specific detection of cytokines. Further studies are required to evaluate the potential benefits of β-TCMP as a bone substitute material.

REFERENCES: [1] E. Landi, G. Logroscino, L. Proietti et al (2008) *J Mat Sci Mater Med* **19**:239-47. [2] R.J. Schutte, A. Parisi-Amon and M. Reichert (2009) *J Biomed Mater Res A* **88**:128-39. [3] M.S. Sader, R.Z. Legeros and G.A. Soares (2009) *J Mat Sci Mater Med* **20**:521-7.

ACKNOWLEDGEMENTS: CNPq, CAPES, FAPERJ and COFECUB.

NANOENCAPSULATION OF ANTIMICROBIAL DRUGS

Jacinthe Gagnon*, and Katharina M. Fromm

Department of Chemistry, University of Fribourg, Chemin du Musée 9, CH-1700 Fribourg, Switzerland
**Corresponding authors: jacinthe.gagnon@unifr.ch; katharina.fromm@unifr.ch*

Silver compounds and nanoparticles are gaining more interest from the scientific society as a replacement to antibiotics. For example, silver compounds may be used to coat implantable materials in order to prevent biofilm formation and other complications due to the presence of bacteria. However, these compounds may be too soluble and even toxic for the host. Encapsulation might be very advantageous in order to increase the stability and biocompatibility of silver drugs.
In this study, CeO_2 nanocapsules were synthesized by coating polystyrene nanospheres with cerium oxide, followed by burning away the core, as shown in Figure 1.

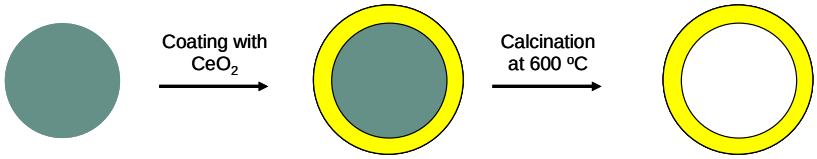

Figure 1: Synthesis of empty CeO_2 nanocapsules

The capsules were then characterized using XRD, TEM and FT-IR. They were then loaded with the silver compound $Ag(L)NO_3$ depicted in Figure 2. For the encapsulation of this compound, $AgNO_3$ and its ligand were inserted in the nanocapsules in two successive steps in such a way that the complexation occurs within the capsule and $Ag(L)NO_3$ remains inside the capsules.

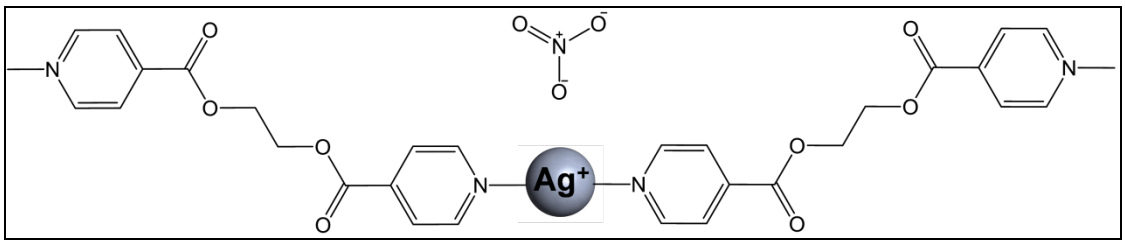

Figure 2: Structure of $Ag(L)NO_3$

The stability in aqueous solutions of the unloaded and loaded nanocapsules as well as their ability to open in presence of a trigger were also investigated.

rhBMP-2: Interactions with Bone Substitute Materials

P.Hänseler[1], E.Fischer[2], C.Mauth[3], R.Schibli[2], F.E.Weber[1]

[1] *University Hospital Zurich, Zurich Switzerland* [2] *Paul Scherre Institute, Villigen, Switzzerland*

[3] *Institut Straumann AG, Basel, Switzerland*

INTRODUCTION: With the expiration of key patents for recombinant human bone morphogenetic protein-2 (rhBMP-2) in the near future, new combinations with established bone substitute materials and/or specific delivery systems will hit the market soon. A key to the design of such devices is the knowledge of the interactions between the bone substitute materials and rhBMP-2. We therefore investigated the interactions between rhBMP-2 and the following clinically evaluated bone substitute materials: a hydrolysable polyethylene glycol (PEG) hydrogel developed as slow release system for growth factors [1] and two apatite based bone substitute materials; deproteinized bovine bone matrix granules (DBBM) [2] and a fully synthetic, porous and biphasic (60:40) hydroxyapatite/tricalcium-phosphate (HA/TCP) scaffold [3].

METHODS: rhBMP-2 was incorporated into hydrogels during gel formation and adsorbed to DBBM and HA/TCP from solution. Samples were immersed in cell culture medium at 37 °C and the concentration profile in the medium was determined by an ELISA during a period of 15 days. Alternatively, rhBMP-2 was labeled with ^{125}I using the Iodogen method. ^{125}I-rhBMP-2 in solution or adsorbed to apatite materials was detected by a gamma counter. Interactions of ^{125}I-rhBMP-2 with PEG were detected by SDS PAGE gels by autoradiography.

After the release, the biological activity of rhBMP-2 in the supernatant was determined in an *in vitro* assay for alkaline phosphatase (ALP) activity, an early marker for osteoblastic differentiation. Stimulation of cells with a sustained release was tested in a perfusion system (Figure 1). Hydrogels and HA/TCP scaffolds were loaded with rhBMP-2 and placed in the reservoir. Released rhBMP-2 was pumped through an HA/TCP scaffold containing uniformly distributed preosteoblastic cells. After an incubation period of 7 days the cells cultured on the scaffold were tested for ALP activity

RESULTS: Release profiles detected by ELISA and gamma radiation showed a sustained release of rhBMP-2 from hydrolysable PEG hydrogels. However, the amount of growth factor detected by ELISA was much lower than in case of gamma radiation. SDS PAGE with autoradiography showed formation of complexes of rhBMP-2 with PEG chains during gel formation. ALP activity stimulated by rhBMP-2 in the supernatant of a terminated release from PEG hydrogels was reduced, but if the cells were stimulated by a sustained release in the perfusion system, ALP activity was raised again. rhBMP-2 showed a high affinity to apatite materials, but it is stronger for DBBM than for biphasic HA/TCP. The biological activity of rhBMP-2 remaining in the supernatant was not affected by the presence of the apatite materials.

DISCUSSION & CONCLUSIONS: High uptake of biologically active rhBMP-2 combined with a slow release is crucial for composite bone substitute materials. Although the bioactivity of rhBMP-2 is affected by the PEG hydrogel, the sustained release is having positive effects on osteoblast differentiation. The high uptake of rhBMP-2 by apatite materials together with the slow release from the hydrogel favors the combination of these materials. But although the presence of apatite materials does not influence the activity of rhBMP-2 remaining in solution, it remains important to know if the adsorbed rhBMP-2 is active or denatured.

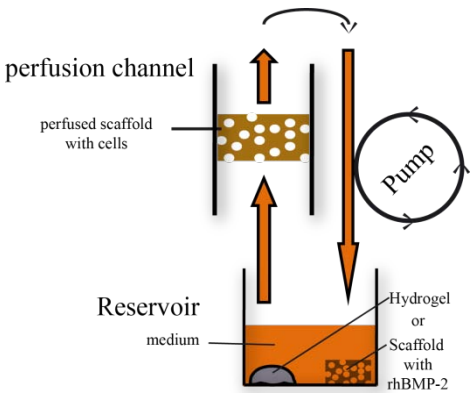

Figure 1: perfusion system

REFERENCES: [1] Jung, R.E., et al., Clin Oral Implants Res, 2009. **20**(2): p. 162-8. [2] Jung, R.E., et al., Clin Oral Implants Res, 2003. **14**(5): p. 556-68. [3] Cordaro, L., et al., Clinical Oral Implants Research, 2008. **19**(8): p. 796-803.

Future dental medicine - Nanodentistry

S.E. Hieber and B. Müller

Biomaterials Science Center, University of Basel, Switzerland

DEFINITION: 'Nanodentistry' is defined as the science and technology of diagnosing, treating and preventing oral and dental disease, relieving pain, and of preserving and improving dental health, using nanoscale-structured materials [1]. The nanotechnology generally considers entities between 1 and 100 nm leading to properties and functionalities of materials that fundamentally differ from what is known from larger scales. The surface of the nanoparticles dominates the materials properties, which are usually given by the bulk.

MATERIALS & METHODS: The common biomaterials are ceramics, metals, and polymers or any kind of combination. Nanoscale patterns on the surfaces and within the volume of the materials accomplish the dedicated functionalities. The fundamental knowledge of the human tissues on the nanometer scale is required to take advantage of these innovative technologies for patients in an efficient manner. Imaging techniques to characterize nanomaterials include micro-tomography, electron microscopy, scanning probe microscopy, X-ray scattering and diffraction methods.

RESULTS: Filling materials for reconstructions, dental root implants, bone augmentation and dentin re-mineralization already take advantage of nanotechnology today, but have increasing growth potential (Fig. 1). Today's dental materials will be replaced by nature-analogue, anisotropic tooth restorations. The nanostructures in dentin are orthogonally oriented to the ones of the same size in the enamel [2]. The calcium phosphate phases for bone augmentation gain more and more importance along with the increase in age of the population. The absorbable calcium phosphate phases or bio-glasses support the growth of the natural bone being applied to larger and larger defects. The materials have to be optimized on the micro- and nanometer scales to tweak the biocompability, the bioactivity and the osseoconductivity promoting tissue regeneration and resisting the mechanical loads. The micro- and nanostructured surfaces of tooth implants guarantee the osseointegration. Nanoparticles are already used in 'sensitive' toothpastes and will enable the re-mineralization of damaged teeth [3].

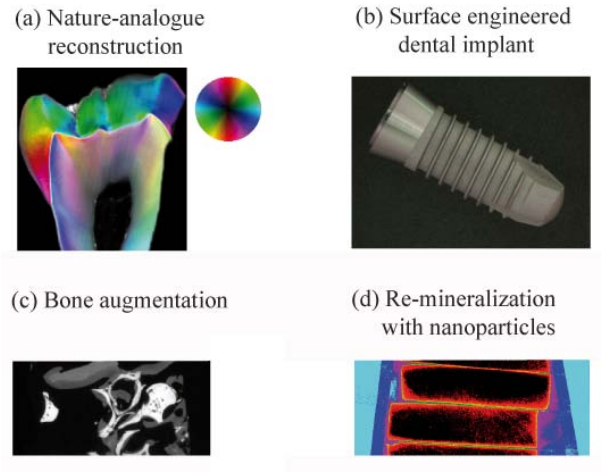

Fig. 1: Present applications of nanotechnology in dentistry with growing turnover.

DISCUSSION: Nanotechnology has started to a new era of dental medicine that will change the current methods in diagnosis, treatment and prevention of the different patients. As medicine advances and people live longer, nanodentistry will play an increasing role in enabling people to keep their natural teeth and oral tissues healthy and functioning. The scientists will understand in detail how the teeth grow, develop and heal. The medical experts will understand the assembly of nanostructures in dentin and enamel to enable the development of biomimetic tooth repair and regeneration. Dentists will be able to reconstruct hard and soft periodontal tissues as well as to treat caries including biomimetic re-mineralization and repair of diseased teeth.

REFERENCES: [1]H. Dosch, M. van de Voorde (Eds.) (2009) *Gennesys White Paper: A new European partnership between nanomaterials science and nanotechnology and synchrotron radiation and neutron facilities.* Max-Planck-Institut für Metallforschung, Stuttgart [2]H. Deyhle et al. (2009). *Bio-inspired dental fillings* Proc. SPIE **7401**:74010E [3]F. Kernen et al. (2008). *Synchrotron radiation-based micro computed tomography in the assessment of dentin de- and re-mineralization* Proc. SPIE **7078**:70780M

ACKNOWLEDGEMENTS: The authors thank H. Deyhle, F. Kernen and F. Schmidli for their contributions to the figure.

Two-layer Membrane of Calcium Phosphate/Collagen/PLGA Nanofibres with a Composition Similar to Bone: in vitro Biomineralisation and Osteogenic Differentiation of Human Mesenchymal Stem Cells

N. Hild, O.D. Schneider, D. Mohn, W.J. Stark
Institute for Chemical and Bioengineering, ETH Zurich, 8093 Zurich, Switzerland.

INTRODUCTION: Guided bone regeneration is one of the present challenges in orthopaedic and dental surgery. Implants need to be osteoinductive and it would be advantageous to have an implant material presenting a chemical composition and a structure as close as possible to those in bone tissue. Dry bone tissue consists of hydroxyapatite (75 wt%) and collagen Type I fibrils (25 wt%). Collagen has a large range of biomedical appliance due to its antigenicity and fibre forming ability. Furthermore, collagen can be used as carrier of bioactive components such as calcium phosphates. The latter are widely used in biomaterials as they are biocompatible, and osteoconductive. In the present study the elaboration of an anisotropic bilayer is described.

METHODS: Amorphous calcium phosphate (a-CaP) nanoparticles, produced by flame spray synthesis, were combined via electrospinning with collagen (Col) Type I and poly(lactide-co-glycolide) (PLGA). The fibres' transformation during crosslinking and biomineralisation was investigated. To obtain a bifunctional membrane dyed a-CaP/Col/PLGA fibres were electrospun on top of pure PLGA. A cell culture study with human mesenchymal stem cells was conducted to analyse differentiation of the cells and exclude any cytotoxic effects of the scaffolds by alamarBlue, alkaline phosphatase activity and confocal laser scanning microscopy. Ca and collagen contents were followed by Alizarin red S and Sirius red staining.

RESULTS: The fibres' morphology depended on the chemical composition. Fibres that contained PLGA were stable enough to undergo crosslinking and biomineralisation experiments. The surface appearance of fibres that contained a-CaP dramatically changed after biomineralisation. The double membrane presented PLGA fibres on its white side and a-CaP/Col/PLGA fibres on the blue side (Fig. 1a-c). *In vitro* proliferation of the cells seeded on the membrane was successful and neither side showed cytotoxicity. Differentiation into the osteogenic lineage was better than in 2D control. Further an augmented content of Ca and collagen was confirmed.

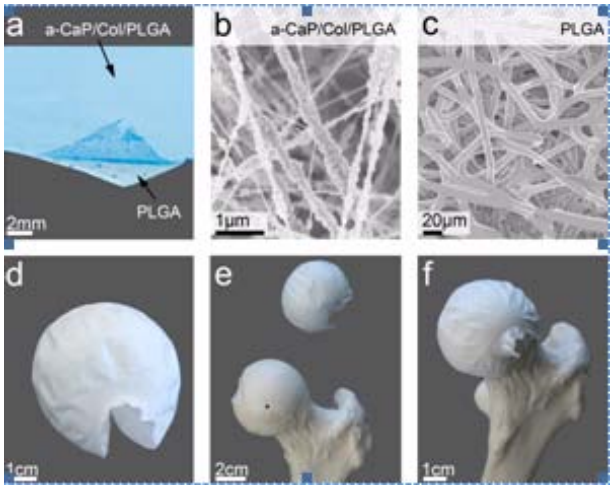

Fig.1 (a) Bilayer with dyed a-CaP/Col/PLGA (SEM in (b)) on one side and PLGA (SEM in (c)) on the other. The bilayer can be electrospun into a spherical shape (d) that can be positioned on a femur head model (e and f).

DISCUSSION & CONCLUSIONS: a-CaP nanoparticles were combined with collagen in a weight ratio similar to the chemical composition of bone tissue and the fibres were strengthened with PLGA. The hydroxyapatite formation indicates the osteoconductivity of the a-CaP-scaffolds. The anisotropic double membrane is easy to handle and can be shaped to be used as a bone wound dressing material. (Fig. 1d-f)

REFERENCES: N. Hild, O.D. Schneider, D. Mohn, N.A. Luechinger, F.M. Koehler, S. Hofmann, J.R. Vetsch, B.W. Thimm, R. Müller, W.J. Stark, (2011) *Nanoscale* **3**:401-409.

Antimicrobial Porous Surfaces for Ti implants

W. Hoffmann[1,3], J. Köser[1], M. de Wild[1], I.Martin[3], F.Schlottig[4], C. Jung[2], U. Pieles[1]
[1]*University of Applied Sciences Northwestern Switzerland, Basel*
[2]*KKS Ultraschall AG Medical Surface Center, Steinen, Switzerland.*
[3]*Department of Biomedicine, Basel, Switzerland*
[4]*Thommen Medical AG, Waldenburg, Switzerland*

INTRODUCTION: Over the last two decades the use of dental implant has been steadily increased with annual growth rates of up to 15%. This has drawn the attention to periimplantitis and poor implant ingrowth as the major causes for implant failure which occurs at a rate of up to 5% [1]. Since the main cause for periimplantitis is the affection of implants with bacteria. Implant surfaces are designed to show antimicrobial activity concurrently to osseoconductive properties.
Here we present results from a multidisciplinary approach to develop new antimicrobial active porous surfaces of titanium implants by spark assisted anodizing. Anodisation offers the unique property to micro- and nanostructure titanium implant surfaces to provide optimal osseo-integration of implants [2] and at the same time to incorporate antimicrobial active metal ions.

METHODS: The surface treatments applied in the course of this project include pre-cleaning, spark-assisted anodizing in proprietary electrolytes and with proprietary anodizing parameters and final cleaning. The spark-assisted anodizing process [3] produces different layers, which can be affected by different post-anodisation treatments. Dilution series of non-adhering bacteria and live/dead staining are performed to assess the antimicrobial activity of the modified surfaces.

RESULTS: It has been discovered that the surface roughness of the anodized layers is very similar for different mechanical pretreatments, as well as the elemental composition of the anodized layers. This demonstrated that the mechanical pretreatment for deburring has no significant effect on the overall anodisation process. Although similar in chemical composition and morphological appearance, the thickness of the porous layer can be tuned, by modifications of the sample preparation protocol under the conditions tested, to 1.5 to 3.5 µm (Fig. 1).

Fig. 1: Scanning electron micrographs of differently modified samples.

The antimicrobial activity of the prepared titanium surfaces has been evaluated a) in extracts obtained after different incubation times of the samples in simulated body fluid as well as b) on the modified titanium samples in direct contact with bacteria.

Next we will establish dedicated live/dead staining protocols to assess the antimicrobial activity of modified titanium surfaces towards biofilm forming bacteria via fluorescent microscopy.

Additionally the biocompatibility of the modified titanium samples was assessed using human bone marrow derived stem cells (Fig. 2).

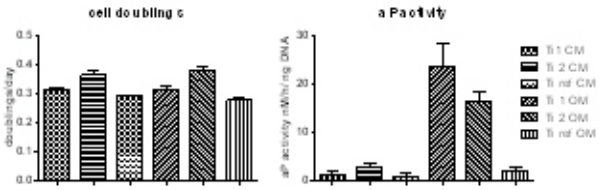

Fig. 2: Stem cell proliferation and alkaline phosphatase activity on various Ti samples in either control medium (CM) or differentiation medium (OM).

DISCUSSION & CONCLUSIONS: Titanium samples were subjected to the electrochemical spark-assisted anodizing process and the layers formed were analyzed with regard to their structural and chemical composition. In initial experiments antimicrobial activity was observed with concurrent biocompatibility and osteoblastic differentiation supporting properties.

REFERENCES:

[1] A. Mombelli, *Microbiology and antimicrobial therapy of peri-implantitis*, Periodontology 2000, Vol. 28, 2002, 177–189. [2] Brunette, et al., *Titanium in Medicine: material science, surface science, engineering, biological responses and medical applications*. Berlin: Springer-Verlag 2001. [3] Jung, C. *Surface properties of titanium implants treated by spark-assisted anodizing*; European Cells and Materials, 2010;19 (Suppl 2):4.

ACKNOWLEDGEMENTS: This research activity belongs to the project “NAPTIS”, funded by the Swiss Nanoscience Institute.

Activity and Long-Term Stability of Self-Assembling Enzymatic Surface Coatings

Sabrina Burgener, Uwe Pieles, and Joachim Köser

University of Applied Sciences Northwestern Switzerland, Muttenz, Switzerland.

INTRODUCTION: Introducing biological and pharmacological active substances to surfaces at the cell materials interface has been a challenge for many years. Recently self assembling processes especially the formation of polyelectrolyte multilayers have gained increased attention for the functionalization of surfaces due to their ease of application, versatility and cost-effectiveness[1]. The concept of polyelectrolyte multilayer functionalization of surfaces relies on the strong cooperative electrostatic interaction of molecules with multiple oppositely charged sidegroups. The principle has been applied to the assembly of multilayer structures from synthetic polymers but also from charged biomolecules such as DNA and proteins. Here we present data on self-assembled enzymatic active surface coatings and discuss the implications of the results for the improvement of medical implant surfaces.

METHODS: The H_2O_2 degrading enzyme catalase was incorporated in multilayer structures on glas surfaces by alternate incubation of the sample surface with enzyme and cationic polyelectrolyte (PEI, polyallylamine, chitosan, Lupamin®) solutions. Subsequently the activity of the immobilized enzyme was quantified by a photometric assay following the catalytic degradation of H_2O_2. The activity and long-term stability of the enzyme harbouring surface coatings was assessed for up to 4 weeks.

RESULTS: For the construction of the bioactive surface coatings presented here we used the enzyme catalase, which has potential applications as a H_2O_2 degrading and anti inflammatory active enzyme on medical implants. With a pI of 5.7 catalase exhibits multiple negative charges at neutral and slightly basic pH and can thus be assembled into alternate multilayer structures with cationic polymers. The built up of multilayer assemblies was proven by comparing the enzymatic activity of structures generated by either two, six or twelve alternate incubations in enzyme and cationic polyelectrolyte (PEI) solutions. Interestingly, if compared to the enzyme in solution the immobilized enzyme exhibited reduced loss of activity upon repeated additions of H_2O_2.

The stability of the enzymatic coating over time was assessed with respect to the polyelectrolyte used for the assembly of the multilayer structure (Fig. 1a) as well as in dependence of the storage pH. Here the highest residual activity of a structure comprising three double-layers of PEI and catalase showed a residual activity of 80% after three weeks storage at pH 8.5 (Fig. 1b). The observed higher residual activity at slightly elevated pH is attributed to the expected increased stability of the multilayer structure when the enzyme exhibits more charges. Thus future work on this topic will deal with the introduction of additional charged groups to the surface of the catalase molecules by simple protein modifications. The knowledge generated from these experiments will further increase the extent of the biochemists toolbox for the optimization of bioactive polyelectrolyte multilayer coatings.

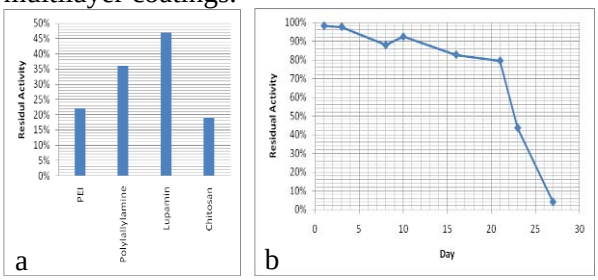

Fig. 1: Residual enzyme activity of multilayer structures composed of catalase and a) different polyelectrolytes after storage for 4 days at neutral pH and b) at pH 8.5 if assembled with PEI.

DISCUSSION & CONCLUSIONS: Here we demonstrate the generation of H_2O_2 degrading enzymatically active surface coatings by self-assembly processes. We determined conditions for the formation and improved long-term stability of the coating and propose approaches for the further optimization of bioactive polyelectrolyte coatings. In summary, our findings support the use of such multilayers as bioactive functionalities during the first few weeks following placement of medical implants.

REFERENCES: [1] Boudou et al. (2010), *Advanced Materials* **22 (4)**, 441-467.

ACKNOWLEDGEMENT: The authors acknowledge the financial support by the Swiss Nanoscience Institute and the help from the members of the Prof. Uwe Pieles group at the FHNW.

Preparation, Characterization and Biological Validation of New Materials for Bone Tissue Engineering Based on Chitosan, Fibroin and Hydroxyapatite

P.A.L.Lima[1,3], D.S.Tavares[2,3], G.D.A.Soares[1,2], L.E.Almeida[1], K.Anselme[3]

[1] UFS / Núcleo de Materiais, São Cristóvão (SE), Brazil. [2] UFRJ / PEMM, Rio de Janeiro (RJ), Brazil. [3] IS2M / IS2M, Mulhouse (MHL), France.

INTRODUCTION: Hybrid composites with chitosan (CHI), fibroin (SF) and hydroxyapatite (HA) are attractive for bone engineering applications but there are very few studies on them in the literature[1,2]. These composites in scaffolds form could be applied as bone substitute in non-loading bearing areas in tissue engineering[3]. The objective of this work was to evaluate *in vitro* Stro+1A cells behavior in contact with CHI, CHI-SF and CHI-SF-HA composites porous scaffolds.

METHODS: The scaffolds were produced from a chitosan solution (2%wt) with SF powder (2%wt) or with SF powder (1%wt) and HA powder (1%wt) in acetic acid. This solution was molded and frozen, and the scaffolds were freeze-dried, crosslinked and submitted to *in vitro* tests with Stro+1A cells under static conditions for 7, 14 and 21 days, with an inoculation density of $5x10^5$ cells. The scaffolds were characterized through X-ray diffraction (XRD), infrared spectroscopy (FTIR) and scanning electron microscopy/energy dispersive spectroscopy (SEM/EDS). Cell viability and activity was assessed by MTT reduction and alkaline phosphate (ALP) activity detection. Student's test was used with a significance at $p<0,05$.

RESULTS: Patterns of XRD showed characteristic peaks at 8.8°, 20.3° and 24.6° (corresponding to SF) and peaks at 31.8°, 32.2° and 32.9° (corresponding to HA). The FTIR presented characteristic bands of the amide groups (SF) and bands of the groups PO^{-3}_4 and CO^{-2}_3 (HA). The EDS showed the presence of the C, O, N, P and Ca elements. SEM analyses indicated cell growth across the surface of the samples. MTT assay showed an increase of the cell number in all scaffolds and the ALP activity was higher in all samples tested at 14 days.

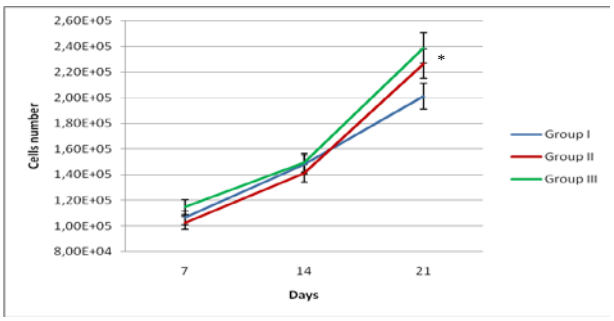

Fig. 1: MTT assay.
** Significantly different than group I (p<0.05).*

Fig. 2: ALP activity.

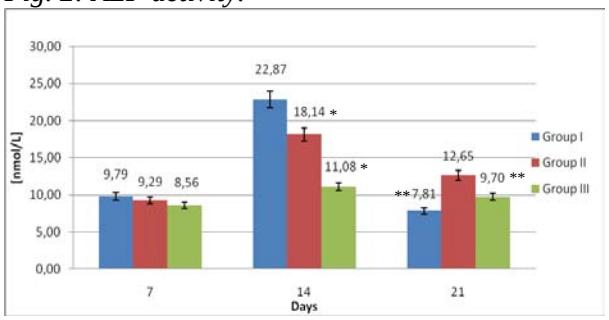

** Significantly different than group I (p<0.05).*
*** Significantly different than group I (p<0.05).*

DISCUSSION & CONCLUSIONS: Despite the fact that SEM analyses indicated cell growth in all the samples, the best behavior was verified in CHI-SF-HA and CHI-SF scaffolds, since they presented a significant higher cell proliferation rate. ALP activity was higher at 14 days than at 7 days and was significant higher on samples of CHI group. After 21 days, the activity decreased for all groups and the best behavior was observed for CHI-SF samples. Likewise, ALP activity represents a marker of osteoblast differentiation, and its decrease after 21 days could represent maturation to osteocytes, which normally express small quantities of enzyme. These initial results indicate that all the materials are not cytotoxic. Molecular studies are under progress to evaluate more deeply the biocompatibility as well as dynamic studies in bioreactors in order to improve cell colonization inside scaffolds.

REFERENCES: [1] Z. She, B. Zhang, C. Jin *et al.* (2008). *Polymer Degradation and Stability*, **93**, 1316-22. [2] L. Wang, Chunzhong, L. (2007). *Carbohydrate Polymers*, **68**, 740-5. [3] W.W. Thein-Han, Y. Kitiyanant, R.D.K. Misra (2008) *Material Science Technology*, **24**, 1062-75.

ACKNOWLEDGEMENTS: CNPq, CAPES, FAPERJ and COFECUB.

Ag-containing plasma polymer coatings with antibacterial and cytocompatible properties

S.Lischer[1], E. Körner[1], D.J. Balazs[1], D. Shen[2], P. Wick[1], K. Grieder[1], D. Haas[2], M. Heuberger[1], D. Hegemann[1]

[1] *Empa, Swiss Federal Laboratories for Materials Science & Technology, Lerchenfeldstr. 5, CH-9014 St. Gallen*

[2] *Department of Fundamental Microbiology, University of Lausanne, CH-1015 Lausanne*

INTRODUCTION: The plasma-coating technology is well established and can be used to create customized surfaces on different materials like implants or catheters. Implants having an antibacterial coating could help to reduce infections that still occur in 1-2% of cases after a total hip arthroplasties [1,2]. Coatings that are used for implants should promote cell growth and provide antibacterial properties. Therefore we investigated plasma polymer coatings containing Ag nanoparticles that provide a release of Ag ions to inhibit bacterial colonization. A further advantage of these nanocomposite thin films is the possibility to tune the surface properties of the plasma polymer matrix to promote cell attachment and proliferation (through the incorporation of amine groups, for instance).

METHODS: Ag-containing and Ag-free amine-rich plasma polymer (a-C:H:N) coatings were deposited in a custom-built modular plasma reactor system. For the Ag-containing films, the metal was sputtered from a Ag cathode introduced in the plasma chamber (asymmetric set-up), in contrast to Ag-free a-C:H:N plasma polymers that were produced in a symmetric set-up. The plasma exposure time was adjusted to deposit coatings of 25 nm thickness. Gas mixtures of variable NH_3/C_2H_4 ratios (2:1 and 4:1) were used with varying power input ranging from 8 to 50 W at a fixed process pressure of 10 Pa. The Ag release kinetic into deionized water was analysed by inductively coupled plasma-optical emission spectrometry. To investigate the antibacterial activity of the coatings, two bacteria strains *S. aureus* (Gram-positive) and *P. aeruginosa* (Gram-negative) were tested. The *in vitro* cytotoxicity assay is based on the ISO-10993-5 and quantified by MTT and DNA assay. The actin and vinculin staining were used to analyse the cell architecture on the coatings.

RESULTS: The amount of Ag and the matrix properties of the nanocomposites are determined by the power input as well as the gas ratio.

The Ag release kinetics over 14 days revealed a fast release within the first 24h, followed by a much slower release. The highest overall release occurred for coatings deposited at higher power input. The reduction of the bacterial colonization on Ag/a-C:H:N-coated surfaces also varied with the power input. Interestingly, the coatings deposited at a relatively low power of 8W were more effective against *P.aeruginosa* than against *S. aureus*. Coatings that were pre-incubated in H_2O for one day showed a significant decrease of the antibacterial effectiveness. In this case, only the coatings with the highest amount of Ag still exhibited antibacterial activity. This shows that the coatings provide a good short-term antimicrobial effect, while a longer-term effect necssitates coatings with higher Ag incorporation. For the cytotoxicity assay the nanocomposite coatings were pre-incubated with cell culture media for 24h. The staining of the cell architecture showed that the Ag-free a-C:H:N matrix is cytocompatible. Light microscopy and quantitative analysis revealed that the increase of power input decreases the cell proliferation and activity on the substrate. However, a high cell activity could be observed on the films deposited at 8W.

CONCLUSIONS: This work demonstrated the use of a co-sputtering plasma polymerization process for the deposition of nanocomposite thin films having a controlled Ag release. By adjusting the coating parameters like the gas ratio and the power input, it is possible to produce biomaterial surfaces with antibacterial and cytocompatible properties.

REFERENCES: [1]Anagnostakos, K. et al, (2009) Classification of hip joint infections. *Int. J. Med. Sci. 6, 227-233.*[2] Fink, B et al., (2009) Revision of late periprosthetic infections of total hip endoprostheses: pros and cons of different concepts. *Int. J. Med. Sci. 6, 287-295.*

Initial Bioadhesion on Surfaces in the Oral Cavity

C. Müller[1], J. Wald[1,2], N. Körber[1], D. Scholz[1], A. Lüders[1], M. Wahl[2], W. Hoth-Hannig[3], M. Hannig[3], M. Kopnarski[2], C. Ziegler[1,2]

[1] Department of Physics and Research Center OPTIMAS; University of Kaiserslautern; D-67663 Kaiserslautern
[2]Institute of Surface and Thin Film Analysis (IFOS) GmbH; D-67663 Kaiserslautern
[3]University Hospital of the Saarland; Department of Operative Dentistry and Periodontology; D-66421 Homburg

INTRODUCTION: On dental materials, the adsorption of proteins and other macromolecules from the saliva on the natural enamel or dental implant material leads to the formation of a biological, bacterial free layer called pellicle. It plays an important role in the formation of a three-dimensional bacterial biofilm on teeth or dental materials and has thus significant relevance for the development of plaque and caries. Although the involved proteins are principally known, there is little knowledge on the basic principles which influence the formation of a protein layer on a molecular scale.
In this context, the adsorption of two of the involved proteins (albumin, lysozyme) on different dental materials were studied by a combined surface analytical approach in which important parameters such as adhesion forces, adsorbed protein amounts, enzymatic activity or reversibility of protein attachment could be derived as a function of parameters such as hydrophobicity and electrostatics. This led to a more detailed understanding of the underlying principles of protein adsorption, pellicle formation, and the consequences for caries and plaque.

METHODS: Protein adhesion and adsorption were investigated with scanning force microscopy (SFM), scanning force spectroscopy (SFS), zetapotential measurements, dynamic contact angle measurements (Wilhelmy plate method; DCA), enzymatic activity and time-of-flight secondary ion mass spectrometry (ToF-SIMS). Investigated substrates were natural enamel, titanium, PTFE, PMMA, ceramic, composite, and dental gold; all prepared to present clinically relevant surfaces.

RESULTS: By means of SFS, adhesion forces up to the piconewton regime were measured between a protein coupled to the SFS cantilever and pure surfaces [1]. The measured adhesion force vs. contact time curves between albumin and the pure surfaces follow a kinetic model in which the protein undergoes a conformational change after the initial adsorption. Equilibrium is reached after a few seconds. Zetapotential measurements revealed the point of zero charge (pH value) for all surfaces [1]. By changing the pH, different electrostatic forces between proteins and surfaces can be established. For BSA, the overall adsorption is dominated by electrostatic forces, only at very basic pH also conformational changes play a significant role. Surfaces with different hydrophobicity show a general trend of higher adhesion forces for more hydrophobic surfaces.
DCA experiments give the amount of adsorbed protein and allow to study the reversibility of the free protein adsorption [2]. Especially for lysozyme a high reversibility was observed on the dental implant materials. It is not possible to wash the BSA completely away. A basical layer stays on the surface. But on the natural enamel both proteins show a high reversibility. The combination of DCA with enzymatic activity measurements shows a high adsorbed amount of albumin and lysozyme for carious conditions (about pH 4,50) attended by a decrease of lysozyme activity.
As a further method, ToF-SIMS gives the lateral chemical composition of the adsorbed protein layer and its homogeneity [3]. Coadsorption and consecutive adsorption studies of two or three proteins reveal competition and displacement processes on the surfaces which are of great importance in the complex in-vivo situation.

REFERENCES:

[1] C. Müller, A. Lüders, W. Hoth-Hannig, M. Hannig, C. Ziegler (2010). Langmuir 26, 4136-4141.
[2] C. Müller, J. Wald, W. Hoth-Hannig, M. Hannig, C. Ziegler (2010). Anal Bioanal Chem, accepted.
[3] J. Wald, C. Müller, M. Wahl, W. Hoth-Hannig, M. Hannig, M. Kopnarski, C. Ziegler (2010). Physica Status Solidi A207, 831-836.

MICROEMULSION APPROACH TO NANOCONTAINERS

Magdalena Priebe*, Katharina M. Fromm

Department of Chemistry, University of Fribourg, Chemin du Musée 9, CH-1700 Fribourg, Switzerland
**Corresponding author: magdalena.priebe@unifr.ch*

ABSTRACT

Within recent years nanometer-sized hollow spheres, called nanocontainers, have attracted increasing interest due to their ability to enclose guest molecules inside their empty core.[1] Because of this potential, hollow nanoparticles may find numerous applications such as drug carriers, reactors, confined reaction vessels, building blocks for photonic crystals or multi-enzyme biocatalysis.[1,2]

The microemulsion approach for the production of nanocontainers is a relatively new method, which allows the preparation of nano-scale hollow spheres without using a solid template. In this case, its role is taken over by a micellar system enabling dissolution of any substance in its core. Subsequent reaction between reagents on the boundary phase between a micelle and the surrounding phase leads to the formation of a nanocontainer.[3,4,5]

The aim of this study is to encapsulate an antimicrobial silver coordination polymer inside inorganic nanocapsules. We have successfully synthesized CuS hollow spheres of a well-defined porous shape using a water-in-oil micellar system. The nanocontainers as well as the encapsulation process were characterized using HRSEM, TEM, EDX, ICP, XRPD and FT-IR methods. Moreover, the stability during long-term storage was investigated.

REFERENCES

[1] Meier W. *Chemical Society Reviews* **2000**, 29, 295–303.
[2] Caruso F. *Advanced materials* **2001**, 13, 11-22.
[3] Feldmann C. et al. *Nanoletters* **2007**, 7, 3489-3492.
[4] Feldmann C. et al. *Small* **2007**, 3,1347 – 1349.
[5] Feldmann C. et al. *Advanced Materials* **2009**, 21, 1586-1590.

Toward Multifaceted Biomaterials that Guide Stem Cell Behaviour: Injectable, Bioactive Hyaluronan-based Hydrogel Scaffolds

R Seelbach[1,2], M Peroglio[1], P Fransen[3], M Royo[3], A Mata[2], M Alini[1], and D Eglin[1]*

[1]AO Research Institute (ARI), Davos, Switzerland, ryan.seelbach@aofoundation.org
[2] The Nanotechnology Platform (PT)/ Parc Científic Barcelona (PCB), Spain,*
[3]Institute for Research in Biomedicine (IRB)/ PCB, University of Barcelona, Spain*

INTRODUCTION

To improve life quality of an older and more active world population, there is a rising demand to treat cartilage disorders and complications using regenerative cell therapy approaches Using 1,3-dipolar cyclo-addition (CuAAC) to synthesize a hyaluronic acid thermoreversible hydrogel incorporated with dendrimers bearing the RGDS peptide sequences, this study aims to promote cell anchorage within this injectable scaffold. The material syntheses are reported together with preliminary chemical characterization and *in vitro* hMSCs attachment seeded on hydrogel layer compositions.

EXPERIMENTAL METHODS

Syntheses. Hyaluronan propargylamide (HApa) was prepared from hyaluronan Streptococcus equi [1]. The syntheses of azido terminated poly(N-isopropylacrylamide) (N_3-PNIPAM) with Mn equal to 20 x10^3 g.mol^{-1} was performed according to procedures already reported [1]. The following dendrimers were prepared as reported previously [2]: **Dendrimer A** with 4 RGDS peptide groups + 1 azide and **Dendrimer B** with 4 RSGD scrambled groups + 1 azide. The reactivity of the dendrimers toward an alkyne model molecule (propargylamine) in the presence of Cu(I) was assessed. Grafting the N_3-PNIPAM and dendrimers onto HApa was performed in PBS, and reacted using a Cu(I) catalyst. Three types of thermoresponsive hydrogels were synthesized with identical quantities of PNIPAM; **Gel A** with dendrimer A, **Gel B** with dendrimer B and **Gel C** without dendrimers. The theoretical density of RGDS was selected such that the peptide concentration in the final volume was 0.005 mM/ml for both gels, a value within the range suggested by Burdick and Anseth. [3] **In vitro study.** hMSCs (M 1960 P5) were seeded at 20,000 cells/cm^2 on top of a 300 µl hydrogel layer in a 24-well tissue culture plate and supplemented between measurements with 1 ml of α-MEM, 10% FCS, 1% NEAA. Cell activity was quantified by Alamar Blue fluorescence (excitation 590 nm, emission 560 nm) every 48 hours over a 7 day period. Histology was performed by fixing cryosections with 4% paraformaldehyde followed by staining with 1% Toluidine Blue for 5 min, washing in MilliQ water then mounting with 2x Xylene and drying.

RESULTS AND DISCUSSION

^{1}H NMR spectrum of the CuAAC reacted dendrimer A with propargylamine (top) shows a peak at 7.3 ppm due to the reaction with the azide and the disappearance of the alkyne peak at 1.91 ppm compared to unreacted dendrimer A and propargylamine (bottom) (Fig. 1).

Histology sections of the hydrogel grafted with bioactive RGDS revealed possible hMSC spreading on the superficial regions of the gel layers which could indicate cell attachment promotion.

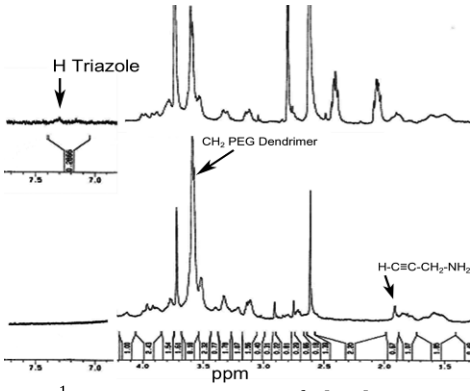

Figure 1: ^{1}H NMR spectrum of dendrimer A in the presence of propargylamine before (bottom) and after (top) CuAAC reaction to verify azide avaibility on dendrimer.

Figure 2: Histology via Toluidine Blue staining of Gel A cryosection in the presence of hMSCs. Scale bar 50 µm.

CONCLUSION

This preliminary study suggests the great potential of the dendrimer nano-technology coupled with efficient hydrogel design for cartilage regenerative therapy. Following study will search to confirm the reported results together with the quantification the actual dendrimer (and RGDS) content within the gel compositions as well as the rheological properties of the gels.

REFERENCES

1. Mortisen, D *et al.*, *Biomacromolecules* **11**, 1261-72 (2010). 2. Pla, D *et al. Bioconjugate Chem.* **20**, 1112-1121. 3. Burdick, J and Anseth, K., *Biomaterials* **23**, 4315–4323 (2002).

ACKNOWLEDGMENTS

The authors would like to thank the PCB and ARI for funding of this research.

Early stages of bacterial biofilm formation – numerical studies of bacterial adhesion on biomaterials

D.Siegismund[1,2], A. Schroeter[2], S. Schuster[2], M. Rettenmayr[1]

[1] *Institute of Materials Science and Technology, Friedrich-Schiller-University Jena, Loebdergraben 32, 07743 Jena, Germany*

[2] *Department of Bioinformatics, Friedrich-Schiller-University Jena, Ernst-Abbe-Platz 2, 07743 Jena, Germany*

INTRODUCTION: The formation of bacterial biofilms plays an important role in nosocomial infections of implants. In the majority of cases such biofilms require a total replacement of the affected implants. The adhesion of bacteria during early stages of biofilm formation is a first crucial step of biofilm formation that is so far only incompletely understood. When an implant is exposed to a medium containing bacteria, the surface properties such as surface energy, surface chemistry and topography control the kinetics of bacterial adhesion. In the present work, a model for bacterial adhesion is introduced that describes early stages of biofilm formation as a function of the surface properties.

METHODS: The model is a further development of our recent Cellular Automaton (CA) model for adsorption of biomolecules on biomaterials[1]. The larger length and time scales relevant for the adsorption of bacteria as compared to proteins require a different treatment of the adhesion energies and in general the thermodynamics of the adsorption process.

In particular, our two-dimensional CA/Finite Difference (FD) adsorption model is combined with the predictions of the extended DLVO (Derjaguin, Landau, Verwey, Overbeek) theory that accounts for the interaction energies between the bacteria and the material's surface. With the combined model, early stages of biofilm formation are simulated.

The model describes the mass transport of bacteria in an aqueous solution towards the material's surface and the adsorption and desorption process depending on the surface properties

RESULTS: The adhesion process of different human pathogenic bacteria (*Enterococcus faecalis, Staphylococcus aureus)* on different biomaterial surfaces (stainless steel, PE, PMMA) has been simulated.

Excellent agreement with experimental findings from the literature concerning the kinetics of the adsorption process is found.

In addition, a realistic bond strengthening mechanism as described by Boks et al.[2] is reproduced by the model.

As an example the calculated bacteria density of *E. faecalis* on the polymeric biomaterial polyethylene as a function of time is shown in Fig. 1.

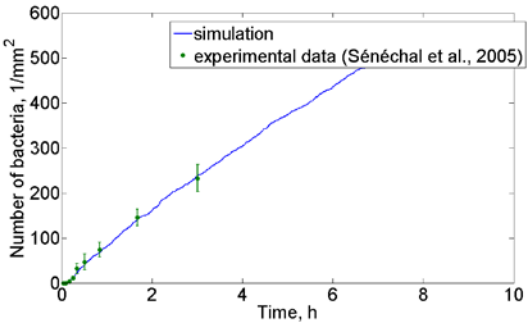

Fig. 1: Adhesion kinetics of E. faecalis on poly-ethylene (PE); simulated curve from this work, experimental values from ref. [3]

The incorporation of the DLVO theory allows describing the significant differences of adsorption on polymeric in contrast to metallic biomaterials.

DISCUSSION & CONCLUSIONS: With the approach for the simulation of bacterial adhesion on biomaterials introduced here, it is possible to characterize the first crucial step of the formation of nosocomial infections of implants. The combination of CA/FD models has the potential to assist the development of implant materials by predicting the adhesion behaviour of bacteria and by allowing the design of more specific experiments.

REFERENCES: [1] D. Siegismund, T. F. Keller, K. D. Jandt, M. Rettenmayr (2010) *Macromol. Biosci.* **10**:1216–23 [2] N. Boks, H. Busscher, H. van der Mei, W. Norde (2008) *Langmuir* **24**:12990-94 [3] A. Sénéchal, C. Catuogno, M. Tabrizian (2005) *J. Biomater. Sci., Polym. Ed.* **16**:115-29

ACKNOWLEDGEMENTS: This work was supported by the Jena School of Microbial Communication (JSMC).

NUCLEIC ACIDS TRANFECTION IN THERMOREVERSIBLE HYALURONAN-BASED GEL

A. Sukarto[1], C. Sapet[2], M. Alini[1], D. Eglin[1]

[1]AO Research Institute, Davos, Switzerland. [2]OZ Biosciences, Marseille, France.

INTRODUCTION: Differentiation of human bone marrow stem cells (hBMSC) in a gel matrix via non-viral vector is desirable in tissue engineering field. It allows continuous differentiation and metabolic activities of hBMSC in a gel and thus functional soft tissue replacement in a host. In addition, non-viral vector offers a better safety profile in clinical settings. Thus, the objective of this work is to investigate the transfection efficiency of hBMSC in thermoreversible hyaluronan gels, grafted with poly(*N*-isopropyl acrylamide) (HA-PNIPAM), using 3D-FectIN™ transfection carrier and secreted alkaline phosphatase (SEAP) encoding plasmid.

METHODS: 0.125 µg pVectOZ-SEAP plasmid (OZ Biosciences, France) were complexed with 0.375 and 0.5 µL 3DFectIN transfection reagent (OZ Biosciences, France), for 20 min. Both SEAP and 3DFectIN were diluted in sterile phosphate buffer saline (PBS), prior to complex formation. 15% w/v HA-PNIPAM in PBS was transferred into eppendorf tubes containing complexes followed by hBMSC with seeding density of 4 x 10^6/ mL. 50 µL of mixed suspension with final concentration of 10% w/v HA-PNIPAM was then added into 48-well plate containing 200 µL media (pre-incubated at 37^0C) and immediately formed crosslinked gels. At each time point (day 1, 3 and 6), 100 µL media was collected, freezed at -20^0C until analysis and replaced with fresh media (α-MEM, 10% Hyclone fetal bovine serum and 1% penicillin-streptomycin). For hBMSC monolayer transfection, similar procedure was performed without HA-PNIPAM gel incorporation. The control for hBMSC transfection on monolayer and in the gels contained 0.5 µL 3DFectIN alone. SEAP production was measured using alkaline phosphatase (ALP) assay, according to the protocol provided by OZ Biosciences, and normalized to deoxyribonucleic acid (DNA) content using Quant-iT™ PicoGreen® dsDNA reagent (Molecular Probes, USA).

RESULTS: Figure 1A showed that ALP secreted by hBMSC in HA-PNIPAM gels was similar to control (0 µg SEAP) for all time points, regardless of reagents ratio (SEAP/ 3DFectIN). In contrast, ALP production was significantly higher for hBMSC transfected in monolayer throughout culture period (Figure 1B). In addition, hBMSC in monolayer culture secreted significantly higher ALP on day 3 when transfected with high ratio of lipoplexes.

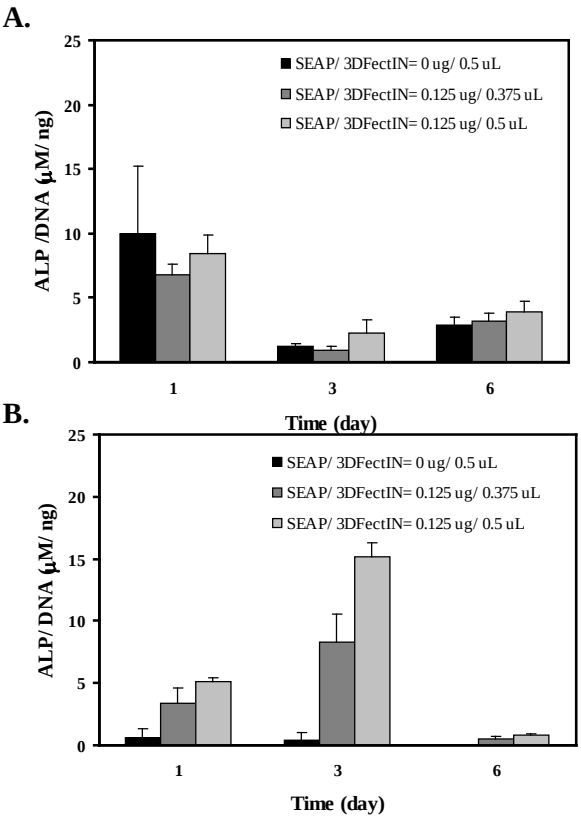

Fig. 1: Production of alkaline phosphatase normalized to DNA content by SEAP-transfected hBMSC in (A) thermoresponsive HA-PNIPAM gels and (B) monolayer culture.

DISCUSSION & CONCLUSIONS: SEAP transfection on hBMSC did not occur in thermoresponsive HA-PNIPAM gels using transfection reagent, but did on monolayer culture. The transfection failure might be attributed to the hydrophobic interactions between PNIPAM chains and the intrinsic transfection carrier formulation.

ACKNOWLEDGEMENTS: We would like to thank OZ Biosciences, France, for kindly providing SEAP plasmid and 3DFectIN™ reagent. This research was supported by the European Union through the FP7 EU-Project: Gene Activated Matrices for Bone and Cartilage Regeneration in Arthritis (GAMBA).

Injection-moulded micro-cantilever arrays for detecting DNA sequences

P. Urwyler[1,2], J. Köser[3], H. Schift[1], J. Gobrecht[1,4], F. Battiston[5], and B. Müller[2]

[1]*Paul Scherrer Institute, Villigen PSI, Switzerland.*
[2]*Biomaterials Science Center, University of Basel, Switzerland.*
[3]*University of Applied Sciences Northwestern Switzerland, Muttenz, Switzerland.*
[4]*University of Applied Sciences Northwestern Switzerland, Windisch, Switzerland.*
[5]*Concentris GmbH, Basel, Switzerland.*

INTRODUCTION: Cantilever sensors detect surface stress created by the interaction of analytes with functional sensor surfaces. Variotherm injection molding technique was employed to fabricate 22 µm-thick polypropylene micro-cantilever arrays. These micro-cantilevers (MC) were functionalised and tested for detecting single-stranded DNA sequences.

METHODS: Variotherm injection molding using metal molds made by laser ablation was applied to fabricate disposable polymeric MC-arrays (see Fig. 1). The cantilevers were coated on one side with 4 nm chromium and 20 nm gold. The array of eight MCs each 500 µm long, 100 µm wide and 22 µm thick was functionalised by means of the Cantisens® FU-401 functionalization unit. The MCs 1, 2, 5, 6 were functionalised with a ss DNA oligonucleotide "Nl4-3" sequence, and MCs 3, 4, 7, 8 with "Sf162". All measurements were done using the Cantisens® Research platform. The experiments were conducted at a temperature of 30 °C, with a constant flow (0.42 µl/s) of a 1M NaCl buffer solution. The sample solution used in this experiment was 1 µM complementary Sf162 diluted in the 1M NaCl.

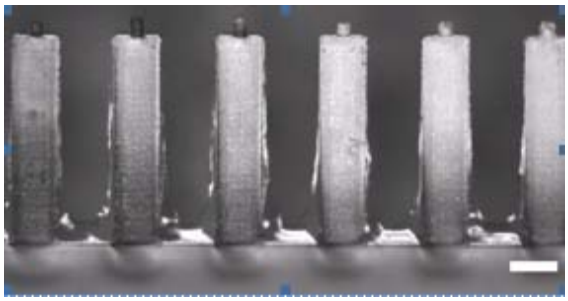

Fig. 1: Optical micrograph of a variotherm injection-moulded polypropylene micro-cantilever array. The scale bar is 100 µm.

RESULTS: The difference of the deflection signals from the reference MCs (1, 2, 5, 6) and the signal MCs (3, 4, 7, 8) is shown in Fig 2. The first sample injection of the complementary Sf162 sequence gives a 7 nm signal, which is comparable to the signals achieved with Si cantilevers.[1] A second injection of the same complementary sequence was a control for saturation from the first injection and led to a 1.5 nm differential signal.

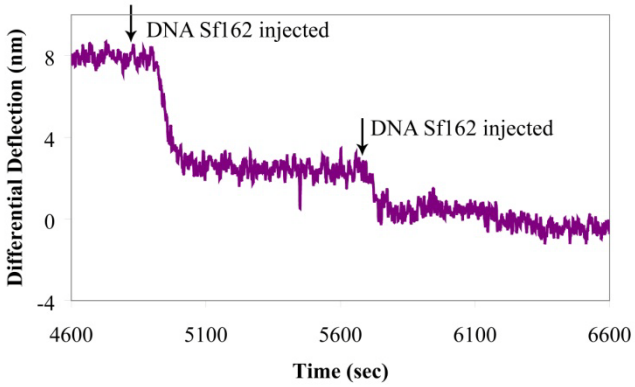

Fig. 2: Deflection upon hybridisation of the complementary sequence.

DISCUSSION & CONCLUSIONS: Polymer micro-cantilever arrays can be used to detect specific DNA sequences. These MCs can be surface structured using the hybrid technology described previously,[2] which can enhance the amplitude of the deflection signal. Surface structuring also enhances cell adhesion and cell spreading, which is vital for further applications including measurement of contractile cell forces,[3] thus opening a wide variety of single-use applications in the field of biomedicine.

REFERENCES: [1]J. Köser, P. Shahgaldian, M. Bammerlin, F. Battiston, U. Pieles (2007) *J. Phys.* **61:**612-617. [2]P. Urwyler, H. Schift, J. Gobrecht, O. Häfeli, M. Altana, F. Battiston, B. Müller (2011) *Sensors and Actuators A* in press. [3]J. Köser, J. Gobrecht, U. Pieles, B. Müller (2008) *Eur. Cells Mater.* **16**:38.

ACKNOWLEDGEMENTS: This activity is funded by the Swiss Nanoscience Institute through the applied research project DICANS. We thank the members from the LMN-PSI, INKA, FHNW (especially O. Häfeli), and EMPA (especially K. Jefimovs) for their technical assistance.

Building Materials from Artificial Phospholipids

P.-L. Zaffalon[1], I. A. Fedotenko[1], A. Zumbuehl[1]

[1] *Department of Organic Chemistry, University of Geneva, Geneva, Switzerland.*

INTRODUCTION: Our group is interested in the organic synthesis of new phospholipids, their biophysical characterization and applications in medicine.[1]

Nature is providing a wealth of thousands of chemically distinct lipid structures. However, a closer look at glycerophospholipids and sphingolipids reveals that this variety is mainly based on combinations of different head groups and tails. The backbone holding together the hydrophilic and hydrophobic parts is conserved and consists either of glycerol or 2-amino-1,3-propanol. Expanding the set of available backbone structures could allow chemistries that are not possible with natural phospholipids.

We have recently introduced a 1,3-diaminopropanol backbone leading to diamido- and diaminophospholipids. Our synthetic strategy is diverse and is based on easily accessible, cheap P(III) and P(V) reagents such as benzyloxydichlorophosphine (BODP) or phosphorodichloridates.[2,3]

We reasoned that structures build from artificial phospholipids, due to the similarity to natural phospholipids, would be interesting candidates for biocompatible materials. Here we like to report our latest progress in the field of polymerizable phospholipids.

METHODS: A 1,3-diaminophosphocholine was synthesized containing two acrylamide functionalities.[4]

Large unilamellar vesicles (100 nm diameter) were prepared from a thin film of lipids. The film was hydrated with buffer at a concentration of 10 mg lipid per 500 µL buffer (107 mM NaCl, 10 mM HEPES, pH=7.4), submitted to 5 freeze-thaw cycles and extruded 11 times through 100 nm filters at 60 °C.

We then deposited an aliquot of 18 µL of the vesicle suspension onto a scanning electron microscopy aluminum stub fitted with double-sided carbon tape. To this was added 2 µL of Irgacure 2959 and the aluminum stub was placed under a 100 W UV light (365 nm) for 15 min. The polymerized material was then washed with pure water and left to dry before it was gold-coated and studied under SEM conditions (see figure 1).

RESULTS: Single 100 nm vesicles were formulated from a polymerizable phospholipid. Upon UV irradiation in the presence of a radical initiator, the vesicles did not polymerize into single, 100 nm structures but into large aggregates of roughly 200 µm. It was shown that the interior of the particles still contains crosslinked vesicles with water-filled cavities. The system thus can be called a vesosome-like structure (vesicles inside vesicles).

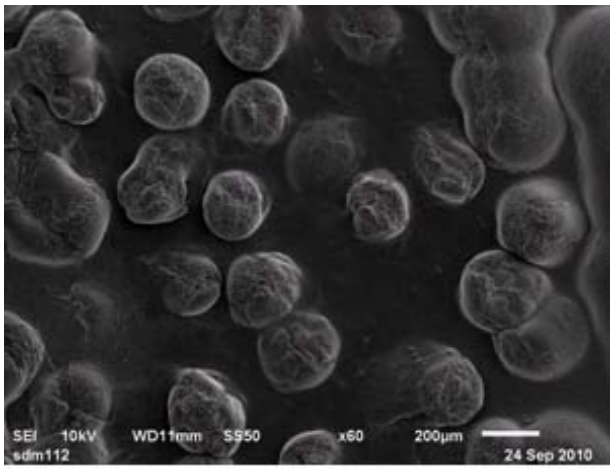

Fig. 1: Single vesicles (100 nm) were polymerized into large aggregates of vesicles

DISCUSSION & CONCLUSIONS: A highly flexible system has been reported: The vesosome-like structure is build from single vesicles that can be formulated from different lipid mixtures. If the vesicles contain non polymerizable phospholipids, the molecules can be extracted from the final polymer using chloroform, leaving behind a holey structure with intersting applications in medicine.

REFERENCES: [1]A. Zumbuehl (2009) *Chimia* **1***:* 63–65. [2]I. A. Fedotenko, P.-L. Zaffalon, F. Favarger, A. Zumbuehl (2010) *Tetrahedron Lett* **51**:5382-5384. [3]P.-L. Zaffalon, A. Zumbuehl (2011) *Synthesis*:778-782. [4]P.-L. Zaffalon, I. A. Fedotenko, E. Stalder, F. Favarger, A. Zumbuehl *paper submitted.*

ACKNOWLEDGEMENTS: The authors thank the Swiss National Science Foundation for financial support.

Mechanical, thermal and rheological properties of acrylic bone cement modified with bone marrow

D. Arens[1], S. Rothstock[1], M. Windolf[1], B. Gueorguiev[1], A. Boger[2]

[1]*AO Research Institute, Davos, Switzerland*

[2] *Synthes GmbH, R&D Biomaterials, Oberdorf, Switzerland*

INTRODUCTION: The use of polymethyl-methacrylate (PMMA) to reinforce fragile or broken vertebral bodies (vertebroplasty) leads to extensive bone stiffening. This might be one reason for fractures at the adjacent vertebrae following this procedure. PMMA with a reduced Young's Modulus may be more suitable. The goal of this study was to produce and characterize PMMA bone cements with reduced Young's Modulus using bone marrow.

METHODS: Bone marrow for modification of the regular cement was harvested from three skeletally mature female Swiss Alpine sheep. Three different compositions of regular acrylic cement modified by different amounts of bone marrow (2.5 ml, 5.0 ml and 7.5 ml) were selected and compared to the regular cement as control (Figure 1). The composites were prepared by manually mixing the bone marrow into the premixed fluid PMMA using the Vertecem V+ mixer and filled into cylindrical Teflon molds (30 mm height, 10 mm diameter).
Cement viscosity, polymerization temperature, setting time, Young's Modulus and Yield strength of different cement modifications were investigated.
Viscosity was measured using 3 ml of the freshly prepared cement placed in a rotational rheometer (Viscosafe Viscometer, Anton Paar, Graz, Austria) according to the method described in a previous study (Boger et al., 2009). Maximum cement temperature and setting time were measured according to ISO 5833. Setting time is defined as the time after start of mixing the cement, when the temperature of the cement is exactly between ambient and peak temperature. The cement was injected into a Teflon mold (6 mm height, 60 mm diameter) and the temperature was measured using a TC-08 thermocouple data logger (PICO Technology, St Neots, U.K.). The cement and the test equipment were maintained at 23 ± 1°C and at a relative humidity of not less than 40% at least 2 h before and during testing. A quasi-static compression test was performed on the cylindrical samples (Figure 1) according to ISO 5833 using an Instron 4302 machine with a compression speed of 5 mm/min and a 10 kN load cell. Young's Modulus and Yield-strength were determined according to the standard and known methods (Boger et al., 2008).

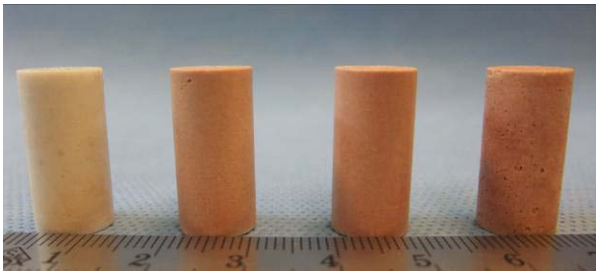

Fig 1: PMMA samples with increasing amount of bone marrow. Left to right: 0.0, 2.5, 5.0, 7.5 ml.

RESULTS:

Table 1 summarizes the results for all parameters of interest (at least three samples per group (n=3)).

Table 1: Results for all parameters of interest as mean and standard deviation.

Bone Marrow content per Vertecem V+ batch [ml]				
	0	2.5	5	7.5
Initial viscosity / Pa*s	123 ± 15	226 ± 26	194 ± 43	208 ± 73
Hardening time /min	25 ± 0.5	15 ± 0.9	17 ± 0.8	19 ± 0.8
Tmax / °C	60.85 ± 2.5	60.7 ± 7.2	42.3 ± 3.2	38.0 ± 4.4
Tset / min	28.3 ± 0.7	16.4 ± 3.3	20 ± 1	24.8 ± 1
Young's Modulus / MPa	1833 ± 47	1283 ± 75	896 ± 76	737 ± 82
Yield strength / MPa	58 ± 4	37 ± 2	26 ± 2	23 ± 1

DISCUSSION & CONCLUSIONS: Blending freshly harvested bone marrow into PMMA cement combines several advantageous effects, like higher initial viscosity, lower polymerization temperature, mechanical properties closer to physiologic values, and high potential of increased bioactivity, all resulting from an easy applicable method. This could potentially be useful for augmentation of osteoporotic cancellous bone.

REFERENCES: 1) A. Boger, K.D. Wheeler, B. Schenk, P.F. Heini, (2009) Clinical investi-gations of polymethylmethacrylate cement viscosity during vertebroplasty and related in vitro measurements. Eur. Spine J., pp 1272-278.
2) A. Boger, M. Bohner, P.F. Heini, S. Verrier, E. Schneider, (2008) Properties of an injectable low modulus PMMA bone cement for osteoporotic bone. J. Biomed. Mater. Res. B Appl. Biomater., pp 474-482.

Metal injection moulding of Ti-Nb alloys for implant application

J.-E. Bidaux, C. Closuit, M. Rodriguez-Arbaizar, E. Carreño-Morelli

University of Applied Sciences Western Switzerland, CH-1950 Sion, Switzerland

INTRODUCTION: Some β or near-β titanium alloys containing elements such as niobium, zirconium or tantalum are particularly suitable as implant materials because of their combination of low elastic modulus, high strength, corrosion resistance and excellent biocompatibility[1]. The difficulty to produce complex shapes with these alloys by conventional techniques makes powder technology attractive. This work investigates the fabrication of Ti-Nb parts by metal injection moulding (MIM).

METHODS: Gas atomised Ti (Dv50=21µm, TLS Technik GmbH & Co) and angular Nb (Dv50=41µm, H.C. Starck GmbH) powders (Figure 1) were mixed with polymer binder in a Coperion Werner & Pfleiderer double sigma mixer to form a feedstock. The binder consisted of 55 wt% paraffin wax, 35 wt% low density polyethylene and 10 wt% stearic acid. The binder volume fraction was 40 vol%. Tensile test specimens (ISO 2740) were injection moulded in an Arburg 221K machine. Binder removal was accomplished by solvent debinding in heptane 20h at 50°C followed by thermal debinding in a Nabertherm VHT08-16MO MIM furnace for 2h at 500°C under argon. The parts were sintered 4h at 1300°C under argon. Tensile tests were performed using a Zwick 1475 machine equipped with extensometers. The density of sintered parts was measured by the Archimedes method.

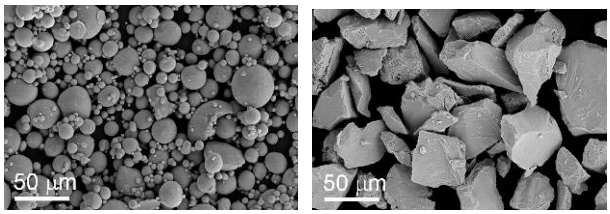

Fig. 1: Scanning electron micrographs showing the base titanium (left) and niobium (right) powders previous to mixing

Fig. 2: Injection moulded and sintered Ti-17%Nb MIM test specimens

RESULTS: Figure 2 shows a green part and a sintered part. The linear shrinkage is about 14%. Good shape preservation and reproducibility has been observed in the set of injection moulded parts. Figure 3 shows tensile test results after sintering at 1300°C. The related mechanical properties are given in Table 1.

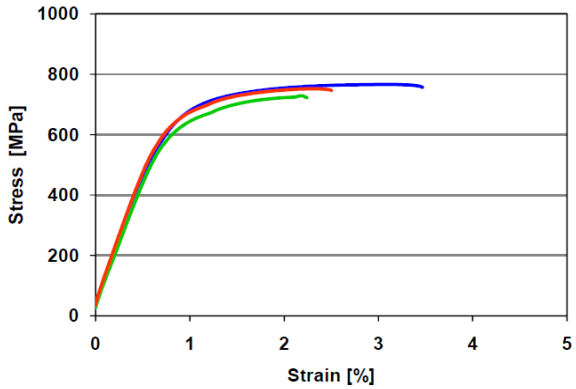

Fig. 3: Tensile behaviour for Ti-17Nb MIM samples sintered at 1300°C

Table 1. Density and mechanical properties of Ti-17Nb MIM samples sintered at 1300°C

PIM alloy	MIM Ti-17wt%Nb
Density (g/cm^3)	4.648 ± 0.013
Elastic modulus (GPa)	83 ± 3
YS (MPa)	652 ± 21
UTS (MPa)	749 ± 19
Elongation (%)	1.9 ± 0.6

DISCUSSION & CONCLUSIONS: MIM Ti-17Nb parts exhibit strengths comparable or better than that of pure titanium[2] but with the advantage of a lower elastic modulus. Low rigidity is important for implants to avoid stress shielding and associated bone resorption. Ongoing research is oriented towards optimisation of the injection moulding and sintering parameters for further increase of strength and ductility. The fabrication of Ti-Nb alloys by MIM is feasible.

REFERENCES: [1] M. Niinomi (2008) *Journal of the mechanical behavior of biomedical materials* **1**: 30-42. [2] E. Carreño-Morelli, W. Krstev, B. Romeira, M. Rodriguez-Arbaizar, H. Girard, J.-E. Bidaux and S. Zachmann (2010) *PIM International* **4**: 60-63.

ACKNOWLEDGEMENTS: The financial support of HES-SO under grant MaCHoP 10-09 is gratefully acknowledged.

Net-shape titanium grade 4 parts processed from titanium hydride powders

E. Carreño-Morelli, M. Rodriguez-Arbaizar, H. Girard, H. Hamdan, J.-E. Bidaux

University of Applied Sciences Western Switzerland, CH-1950 Sion, Switzerland

INTRODUCTION: The fabrication of titanium-based implants and medical devices usually needs several complex steps[1]. Net-shape processing by powder injection moulding (PIM[2]) of titanium hydride powders, which are cheaper and less reactive than titanium powders, can be the solution for breaking the cost barrier[3].

METHODS: Angular TiH_2 powder from AG Materials Inc., Taiwan, was used (Figure 1). The particle size distribution was determined by laser diffractometry in a Malvern Mastersizer 2000 apparatus (median size Dv50 = 20.26 µm).
Feedstocks for PIM were prepared with a binder consisting of 55 wt% paraffin wax (Sigma Aldrich GmbH, Buchs, CH), 35 wt% low density polyethylene (LDPE Riblene MP30, Polimeri Europa, I) and 10 wt% stearic acid (Sigma Aldrich GmbH). The solids loading was 60 vol%. Mixing was performed in a Coperion LUK 1.0 sigma blade mixer (Werner & Pfleiderer, Stuttgart, D) at 140°C for 4h. Polymer-powder granules were obtained by cooling down and crushing the mixture by slow shearing. Tensile test specimens were injection moulded in an Arburg 221K 350-100 machine (Arburg GmbH + Co KG, Lossburg, D).
Green parts were solvent debinded in heptane, then thermal debinded and dehydrided at 500°C under argon. Titanium parts were sintered at 1200°C under argon in a Nabertherm VHT08-16MO MIM furnace. Quantitative analysis was performed by fusion and infrared detection with LECO systems to establish the content of interstitial elements O, N, C in sintered parts. Tensile tests were performed in a Zwick 1475 machine.

RESULTS: Figure 1 shows both green (as injection moulded) and sintered dog bone parts. The shrinkage of about 19% is the result of binder removal and an additional contraction, which occurs during dehydriding of the TiH_2 base powder. The sintered density is 97.1% of the theoretical density.

Fig. 1: Titanium hydride powders, injection moulded and sintered titanium parts

The measured tensile properties are summarized in Figure 2 and Table 1. Together with a low content of interstitial elements (Table 1), the overall performance of PIM titanium meets the requirements of Ti grade 4.

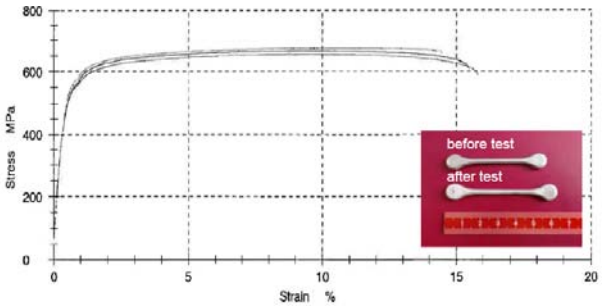

Fig. 2: Tensile behavior of PIM Ti parts from titanium hydride, 4h sintering at 1200°C

Table 1. Interstitial content and mechanical properties of PIM Ti parts from titanium hydride

	O [wt%]	N [wt%]	C [wt%]	density [%]	YS [MPa]	UTS [MPa]	elongation [%]
PIM-Ti	0.30	0.027	0.065	97.1	519	666	15
Ti grade 4	0.4	0.05	0.08	100.0	480	550	15

DISCUSSION & CONCLUSIONS: Titanium hydride powders are an attractive alternative for processing PIM Ti grade 4 parts. Their cost is about 50% of gas atomized Ti powders. Despite its angular shape (which is currently associated with low packing and high interparticle friction) and a necessary dehydriding step, good mechanical properties, shape preservation and reproducibility are achieved. Research is ongoing to evaluate the fatigue properties. PIM of Ti grade 2 parts would be feasible with powders of improved purity and optimized debinding and sintering conditions.

REFERENCES: [1] M. J. Donachie (2000), *Titanium, a technical guide*, Second Edition, ASM International, Materials Park, OH, [2] R. M. German and A. Bose (1997), *Injection Molding of Metals and Ceramics*, MPIF, Princeton, NJ, [3] E. Carreño-Morelli, W. Krstev, B. Romeira, M. Rodriguez-Arbaizar, H. Girard, J.-E. Bidaux and S. Zachmann, *PIM International*, 2010, vol. 4, no. 3, pp. 60-63.

ACKNOWLEDGEMENTS: The technical support of D. Zufferey (HES-SO Valais) and J. Dänzer (BFH-Biel) is gratefully acknowledged.

Biodegradable polylactide/hydroxyapatite nanocomposite foam scaffolds for bone tissue engineering

C.Delabarde, CJG.Plummer, PEB.Bourban, D. Pioletti, JAE.Månson,

EPF Lausanne, Lausanne, Switzerland.

INTRODUCTION: In the USA alone, 0.5 million bone grafts are carried out each year to treat bone loss from fracture or tumors. Our institute is developing new solvent-free processing routes for next-generation resorbable synthetic poly-L-lactide (PLLA)/nano-hydroxyapatite (nHA) bone replacement materials. The approach proposed here is to use highly dispersed PLLA/nHA, in which the modifier particles are comparable in size and composition to those in natural bone, combined with targeted surface treatments as a means of enhancing the osteoconductivity of the scaffolds. The investigation has covered: (i) the preparation, basic structure-property relationships and degradation behavior of the nanocomposites; (ii) the optimization of processing parameters for the production of porous nanocomposite scaffolds by supercritical CO_2 foaming; (iii) the *in vitro* and *in vivo* response of the scaffolds.

RESULTS & DISCUSSIONS: Comparison of various methods for the homogeneous dispersion of the nanoparticles in the PLLA matrix led to the choice of mechanical mixing with a miniature twin screw extruder, which gave excellent degrees of dispersion of nHA without the need for an organic solvent or surfactants. Initial studies of the crystallization behavior of the PLLA/nHA nanocomposites showed nHA addition to result in a decrease in spherulite growth rates but an increase in nucleation density, leading to a significant increase in the global crystallization rates. Addition of nHA particles also resulted in increases in the rate of mass loss during *in vitro* ageing of bulk films, identified with accelerated degradation at the matrix/particle interfaces. However, the tensile strengths and strains to fail were significantly higher in the aged films in the presence of nHA, which suggested the nHA to act as an effective toughener of the bulk material and hence to retard the loss in tensile strength during resorption. Finally, the accelerated ageing treatments used for the degradation tests were found to result in significantly increased hydrophilicity and, in the case of the PLLA/nHA nanocomposites, significant pitting at the scale of the nanoparticles and increased nanoparticle concentrations at the film surfaces, suggesting that such treatments may also be beneficial for the interactions between the nanocomposites and bone cells during implantation.

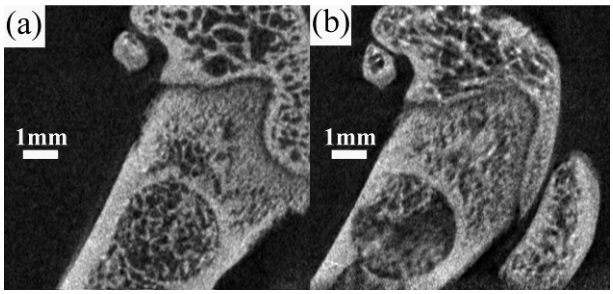

Fig. 1: Micro-CT images of rat femoral condyles with (a) NaOH treated PLLA/10 wt% nHA scaffold, (b) PLLA/5 wt% TCP scaffold, after 8 weeks of implantation.

In foams prepared by supercritical CO_2 processing, the addition of nHA resulted in reduced foam cell sizes and improved homogeneity in the cell size distribution, but did not significantly affect the degree of crystallinity, which remained of the order of 50 wt% in all the foams. Indeed, the compressive modulus and strength were found to be primarily influenced by the porosity of the foams. Even so, the mechanical properties of the foams were comparable with those of trabecular bone, and by adjusting the saturation pressure and depressurization rate it was possible to generate porosities of about 85 %, an interconnected morphology and cell diameters in the range 200-400 µm from PLLA containing 10 wt% nHA, satisfying established geometrical requirements for bone replacement scaffolds. On the basis of the degradation studies and comparison with other potential surface treatments, selected scaffolds were also aged in aqueous NaOH in order to improve cell-scaffold affinity. After 8 weeks of implantation *in vivo* in rat femoral condyles, growth of new bone was confirmed to be significantly enhanced in the NaOH treated PLLA/10 wt% nHA scaffolds, as compared with untreated controls and previous generation scaffolds containing βTCP microparticles (Fig.1). These results are considered to be highly promising, and provide a firm basis for the further development of this technology for clinical implementation.

Shear Stress Sensitive Nanocontainers for Targeted Drug Delivery

M. N. Holme[1,2,3], A. Zumbuehl[1], T. Saxer[2], B. Müller[3]

[1] Department of Organic Chemistry, University of Geneva, Geneva, Switzerland.
[2] University Hospitals of Geneva, Rue Gabrielle-Perret-Gentil 4, Geneva, Switzerland.
[3] Biomaterials Science Center, University of Basel, c/o Universitätsspital, Basel, Switzerland.

INTRODUCTION: Heart attack is the leading global cause of disease and mortality [1]. Ambulatory treatment includes the intravenous administration of vasodilators such as nitroglycerin to restore coronary blood flow at critically constricted arteries and prevent further myocardial ischemia with ensuing arrhythmias and death. Unfortunately, systemic action of these drugs leads to complications such as vasodilation inducing severe hypotension and diminished blood perfusion of the suffering heart.

The lack of biomarkers in these critically constricted arteries demands the development of alternative methods for targeted drug delivery during heart attack. We propose using the body's own changes in shear stress as a purely physical trigger for the release of a vesicle payload. In *in vitro* fluorescence release studies, we investigated the properties of vesicles formulated from certain mixtures of Egg-PC and either the artificial phospholipid Pad-PC-Pad[2], or the surfactant Brij S10.

METHODS: In order to assess the feasibility of drug release from a vesicle through shearing, vesicles of varying formulations were subjected to *in vitro* shear stresses found in physiological hemodynamic flow conditions. 50 mM 5(6)-carboxyfluorescein encapsulated large uni-lamellar vesicles (LUVET100) were prepared by the thin film method [3] from lipid formulations of 30 µmol Egg-PC with Brij S10 added to the lipid mixture in varying concentrations of 0 to 1 mol% in increments of 0.1 mol%. Vesicles with varying compositions (10, 25, 50, 75 and 100 mol%) of Pad-PC-Pad and Egg-PC were prepared by the same thin film method.

To simulate the physical conditions in the heart a model cardiovascular system was used, with vesicles pumped through either a common (shear stress approx. 2 Pa) or constricted (shear stress approx. 10 Pa) model artery constructed from PMMA (Elastrat Sàrl, Switzerland). Both artery models were formed from tubes with an inlet diameter of 2.5 mm, one with constrictions of up to 95% cross sectional area along a 2.5 cm segment. An extracorporeal circulation (ECC) pump (Medtronic Bio-Pump, Bio Console 540, Medtronic, Switzerland) with low intrinsic shear stress simulated the heart [4, 5].

RESULTS: Vesicles formulated from mixtures of the natural phospholipid Egg-PC and 0-1 mol% of the surfactant Polyoxyethylene (10) Stearyl Ether (Brij S10) were found to release up to only an additional 14% of their payload after 40 passes through the constricted artery model, and 3% after 40 passes through a common artery model. This maximum effect was observed in Egg-PC vesicles incorporating 0.5 to 0.6 mol% of Brij S10. These findings build on studies performed by Bernard et al., who found that at shear rates of 10,000 s^{-1} there was a release of contents from Egg-PC vesicles containing 0.1% and 1% Brij S10 [6].

The shear stress-induced release from pure Pad-PC-Pad vesicles is an order of magnitude higher than formulations including Egg-PC. Formulations containing only Pad-PC-Pad were found to release an additional 51% of their payload after one pass through the constricted artery model, whereas in a common artery model only 27% additional release was observed. In both the Pad-PC-Pad and Egg-PC/Brij S10 formulations, background release was around 20%.

Vesicles formulated from mixtures of Pad-PC-Pad and Egg-PC become unstable, or leaky, with an increase in Pad-PC-Pad. Although a higher background release was observed with increased Pad-PC-Pad, they did not significantly increase their susceptibility to shear-induced release.

DISCUSSION & CONCLUSIONS: The results show that the shear-induced release properties of vesicles can be tuned by varying the lipid composition. The Pad-PC-Pad formulation shows great potential for preferential shear-induced release of heart attack drugs near arterial stenoses in the first pass through the blood stream. Investigations are ongoing for the suitability of these and similar non-natural lipid formulations for specificity in drug delivery at elevated shear stresses, for example for cardiac, neurologic or angiologic applications.

REFERENCES: [1] Lopez, A.D., et al., *Lancet*, 2006, **367**(9524), 1747. [2] Fedotenko, I.A., et al., *Tet. Lett.*, 2010, **51**(41), 5382. [3] Olson, F., et al., *BBA*, 1979. **557**(1), 9. [4] Curtis, J.J., et al., *Annal. Thoracic Surg.*, 1999, **68**(2), 666. [5] Paparella, D., et al., *ASAIO J.*, 2004, **50**(5), 473. [6] Bernard, A.L., et al., *J. Coll. & Interfac. Sci.*, 2005, **287**(1), 298.

ACKNOWLEDGEMENTS: The authors thank the Swiss National Science Foundation for financial support.

Plasticization of Poly-L-Lactide with Polyethylene Glycol for Tissue Engineering

M. Cuénoud [1], P-E. Bourban [1], C. J. G. Plummer[1], J-A. E. Månson[1]

[1] *Laboratoire de Technologie des Composites et Polymères (LTC), Ecole Polytechnique Fèdèrale de Lausanne (EPFL), Station 12, Lausanne CH-1015, Switzerland.*

INTRODUCTION: Plasticization of medical grade poly-L-lactide (PLLA) by addition of polyethylene glycol (PEG) with various molar masses has been evaluated as means of producing low stiffness matrices for bioresorbable scaffolds for soft tissue engineering applications[1].

METHODS: Dumbbell-shaped tensile test specimens were obtained by melt-extrusion and melt-injection of various blends of PLLA and PEG using a micro-compounder with twin conical corotating screws (Micro 5 Compounder, DSM, Netherlands). The specimens referred to as ‘‘dry’’ were transferred to a desiccator at room temperature prior to testing. The specimens referred to as ‘‘wet’’ were immersed in a phosphate buffered saline (PBS) solution for 5 days at 37 °C to simulate conditions *in vivo*. The water uptake of the specimens was measured by thermogravitometric analysis (TGA). The tensile behavior and thermal response were investigated using a tensile test machine (UTS, Testsysteme, Germany) and differential scanning calorimetry (DSC Q100, TA instrument, United States).

RESULTS: As reported previously[2], the T_g of injection molded specimens of the PLLA/PEG blends decreased strongly with PEG content (Figure 1). At PEG contents of 15 and 25 wt% it became significantly lower than normal human body temperature, implying an essentially rubber-like mechanical response *in vivo*. The degree of crystallinity of the moldings also increased strongly with PEG content, reaching a maximum of about 60 wt% at 25 wt% PEG. Moreover, after the immersion in PBS for 5 days in 37 °C, the moldings with the highest PEG contents showed increased water uptake and, for relatively low molar mass PEG, significant mass loss, associated with phase separation and leaching of the PEG (Figure 1). Blends with relatively low PEG contents also showed large increases in their degree of crystallinity. The maximum decreases in the elastic moduli at room temperature were limited to about 60% under these conditions, an effect that was attributed both to phase separation and crystallization of the PEG, and to leaching of the PEG at high PEG contents.

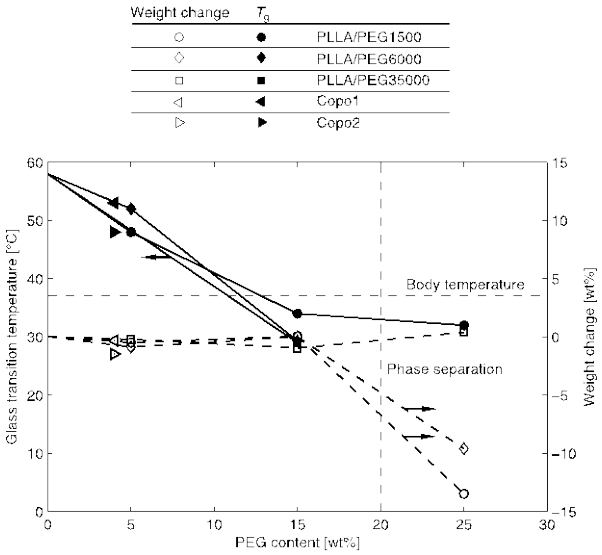

Fig. 1: Glass transition temperature and matrix weight change as a function of the PEG content for the various mouldings.

DISCUSSION & CONCLUSIONS: PLLA/15 wt % PEG35000 was considered to be the most promising candidate for use in soft scaffolds owing to its relatively good stability in PBS at 37 °C (which may be imputed in turn to the relatively high molar mass of the PEG), and its T_g of approximately 34 °C, implying the amorphous content to be in the rubbery state *in vivo*. Blending PLLA with PEG also has the key advantage of facilitating the preparation of materials with continuous mechanical property gradients (by varying the plasticizer content).

REFERENCES: [1]M. Cuénoud, P-E. Bourban, C. J. G. Plummer and J-A. E. Månson (2011) Plasticization of Poly-L-lactide for Tissue Engineering in *Journal of Applied Polymer Science*, article in press.

[2]Y. Hu, Y.S. Hu, V. Topolkaraev, A. Hiltner and E. Baer (2003) Aging of poly(lactide)/poly(ethylene glycol) blends. Part 2. Poly(lactide) with high stereoregularity in *Polymer*, pp 5711-5720.

ACKNOWLEDGEMENTS: We thank Prof. D. P. Pioletti for valuable discussions and the Swiss National Science Foundation for financial support (contract grant number: 205320-121893).

Stress Analysis in MOD Restored Teeth

F. Topală, L. Sandu, S. Porojan

"V. Babes" University of Medicine and Pharmacy Timişoara, Romania.

INTRODUCTION: Cast metal inlays can be used on premolars requiring a MOD restoration instead amalgam and offer a durable alternative. Because it is known that MOD inlays may increase the susceptibility to fracture, it is important to ensure optimal performance in selection of the adequate preparation design to reduce stresses in teeth structures and also in the restorations [1-4]. The aim of the study was to determine the optimal shapes of MOD cast metal inlays in premolars in order to minimize the potentially damaging effects of stress on teeth structures and restorations.

METHODS: The study was performed on an upper first premolar, using a finite element analysis. The 3D model of an unrestored tooth created after laser scaning using a manufactured device. Twenty-two 3D models of maxillary first premolars, with the following designs of MOD ceramic restorations (Fig. 1, 2) were generated: eleven inlays with butt joint margins, eleven onlays with butt joint margins, both with different tapers (between 0 and 10 degree).

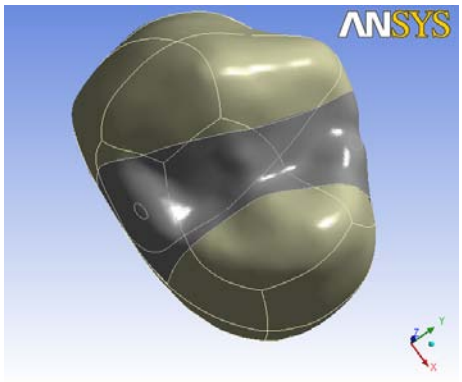

Fig. 1. Geometrical model of the inlay restored premolar.

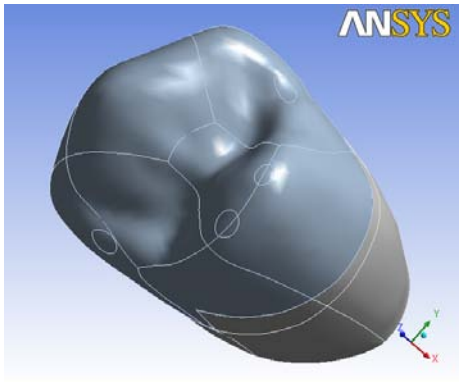

Fig. 2. Geometrical model of the onlay restored premolar.

Computational simulation of an occlusal load of 200 N was conducted, and stresses occurring in the ceramic restorations, and teeth structures were calculated using Ansys finite element analysis software.

RESULTS: Occlusal load on an MOD restored tooth produces stress surrounding the contact areas (Fig. 3). In the teeth restored with ceramic MOD inlays, the von Mises equivalent stress values were higher than in the intact tooth. The stresses were significant lower in all cases when an onlay was used for the MOD restoration compared to those when an inlay was used. The taper of the preparation has no influence on the stress values for all the studied cases.

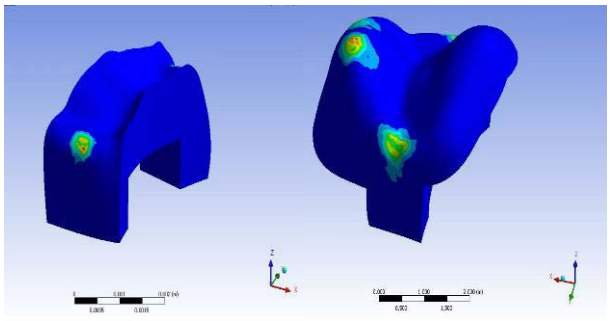

Fig. 3. Stress distribution in restorations.

DISCUSSION & CONCLUSIONS: The MOD restoration on premolars has to distribute the load over a wide surface. Covering the occlusal surface with the restoration, using an MOD onlay, may prevent failure and produce a lower stress values than an MOD inlay.

REFERENCES: [1]P. Ausiello, A. Apicella, C.L. Davidson, S. Rengo (2001), *J Biomech*, 34:1269-77. [2]B. Dejak, A. Mlotkowski, M. Romanowicz (2007) *J Prosthet Dent* 98: 89-100. [3]B. Dejak, A. Mlotkowski (2008) *J Prosthet Dent* 99:131-140. [4]R. B. Fonseca, A.J.F. Neto, L.C. Sobrinho, C.J. Soares (2007), *J Prosthet Dent* 98:277-284.

ACKNOWLEDGEMENTS: This work was supported by CNCSIS-UEFISCSU, project number PN II-RU TE_217/2010.

β TITANIUM ALLOYS AND THEIR INTERACTION WITH BIOLOGICAL TISSUE: THE EXAMPLE OF TOTAL JOINT REPLACEMENT

N. Diomidis[1], N.S. More[2], M. Roy[3], S.N. Paul[2], S. Mischler[1]

[1]*Tribology and Interface Chemistry Group, EPFL, CH-1015 Lausanne, Switzerland.*
[2]*Department of Metallurgical and Materials Engineering, Visvesvaraya National Institute of Technology, Nagpur: 440 011, India.*
[3]*Defence Metallurgical Research Laboratory, Hyderabad: 500 058, India.*

INTRODUCTION: Knee and hip joint replacement implants are immersed in body fluids and involve a sliding contact between the femoral component and the tibial or acetabular component, thus making the metallic parts susceptible to sliding tribocorrosion[1]. Micro-motions occur at the fixation between the implant stem and the bone or cement and are thus subjected to fretting-corrosion[2]. Both of these tribo-electrochemical degradation mechanisms lead to the release of metallic ions and particles in the surrounding tissue. β Titanium alloys are potential biomaterials for joint prostheses due to their biocompatibility and increased compatibility with the mechanical properties of bone.

METHODS: Ti-29Nb-13Ta-4.6Zr alloy with a β microstructure was tested in Hank's balanced salt solution at open circuit potential and at an applied potential in the passive region at 37^0C. Reciprocating sliding tribocorrosion tests were carried out against technical grade ultra high molecular weight polyethylene (UHMWPE) pins with a diameter of 12 mm. The applied load was 6.5 N, at a frequency of 1 Hz, with a stroke length of 5 mm for 3600 s. Fretting-corrosion tests were carried out against alumina balls with a diameter of 10 mm. The applied normal load of was 10 N, with a displacement of 100 µm and a frequency of 1 Hz was applied for 3600 s. The potential and current, the coefficient of friction and the vertical position of the counterbody were measured *in situ*. The wear tracks were characterized by SEM and laser profilometry after the tribological tests.

RESULTS: Under both sliding tribocorrosion and fretting-corrosion the evolution of the electrochemical parameters is indicative of the surface state of the material (Fig. 1). The potential drops indicating a depassivation of the surface as soon as sliding is imposed. The current increases due to the oxidation of the uncovered base alloys. The electrochemical parameters during sliding and fretting regain the values measured before the onset of the motion indicative of passivity recovery despite the mechanical perturbation. The ability of an alloy to regain its passive state while sliding is a critical property in biomedical prosthetics applications since the release of metallic ions due to wear-accelerated corrosion will be limited during the lifetime of the artificial joint.

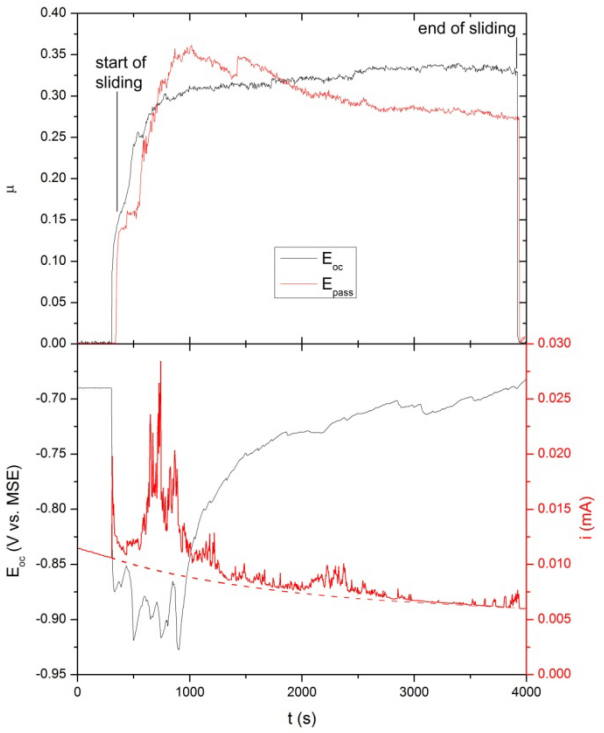

Fig. 1: Evolution of the coefficient of friction (top), open circuit potential and anodic current (bottom) during sliding tribocorrosion testing on Ti-29Nb-13Ta-4.6Zr.

DISCUSSION & CONCLUSIONS: Ti-29Nb-13Ta-4.6Zr regains its passive state during sliding and fretting irrespective of potential. No wear of the Ti alloy is measured when sliding against UHMWPE, while the wear of UHMWPE depends on electrochemical conditions during sliding. Wear of the Ti alloy is measured when fretting against Al_2O_3. Different depassivation and wear mechanisms prevail under sliding tribocorrosion and fretting-corrosion

REFERENCES: [1]N.S. More, N. Diomidis, S.N. Paul, M. Roy, S. Mischler, *Materials Science and Engineering C*, 31 (2011) 400-408. [2]N. Diomidis, N.S. More, S.N. Paul, M. Roy, S. Mischler, *Wear, in press.*